AGU PUBLICATIONS

Geochemistry, Geophysics, Geosystems

RESEARCH ARTICLE

10.1002/2017GC007212

Key Points:
- Lower crustal strength controls the onset and amount of melting and serpentinization during 'ultra-slow' continental rifting
- Strong lower crust favors a continent-ocean transition with exhumed and serpentinized mantle, underlain by frozen magma
- Weak lower crust favors a magmatic dominated COT, perhaps underlain by serpentinites

Supporting Information:
- Supporting Information S1
- Movie S1
- Movie S2
- Movie S3
- Movie S4
- Movie S5

Correspondence to:
E. Ros,
Elena.Ros.2014@live.rhul.ac.uk

Citation:
Ros, E., Pérez-Gussinyé, M., Araújo, M., Thoaldo Romeiro, M., Andrés-Martínez, M., & Morgan, J. P. (2017). Lower crustal strength controls on melting and serpentinization at magma-poor margins: potential implications for the South Atlantic. *Geochemistry, Geophysics, Geosystems*, *18*, 4538–4557. https://doi.org/10.1002/2017GC007212

Received 31 AUG 2017
Accepted 14 NOV 2017
Accepted article online 2 DEC 2017
Published online 21 DEC 2017

Lower Crustal Strength Controls on Melting and Serpentinization at Magma-Poor Margins: Potential Implications for the South Atlantic

Elena Ros[1], Marta Pérez-Gussinyé[2], Mario Araújo[3], Marco Thoaldo Romeiro[3], Miguel Andrés-Martínez[2], and Jason P. Morgan[1]

[1]COMPASS, Department of Earth Sciences, Royal Holloway University of London, Egham, UK, [2]MARUM – Center for Marine Environmental Sciences, University of Bremen, Germany, [3]Petrobras R&D Center, Horácio Macedo Avenue, 950, Rio de Janeiro, Brazil

Abstract Rifted continental margins may present a predominantly magmatic continent-ocean transition (COT), or one characterized by large exposures of serpentinized mantle. In this study we use numerical modeling to show the importance of the lower crustal strength in controlling the amount and onset of melting and serpentinization during rifting. We propose that the relative timing between both events controls the nature of the COT. Numerical experiments for half-extension velocities $<=10$ mm/yr suggest there is a genetic link between margin tectonic style and COT nature that strongly depends on the lower crustal strength. Our results imply that very slow extension velocities ($<$ 5 mm/yr) and a strong lower crust lead to margins characterized by large oceanward dipping faults, strong syn-rift subsidence and abrupt crustal tapering beneath the continental shelf. These margins can be either narrow symmetric or asymmetric and present a COT with exhumed serpentinized mantle underlain by some magmatic products. In contrast, a weak lower crust promotes margins with a gentle crustal tapering, small faults dipping both ocean- and landward and small syn-rift subsidence. Their COT is predominantly magmatic at any ultra-slow extension velocity and perhaps underlain by some serpentinized mantle. These margins can also be either symmetric or asymmetric. Our models predict that magmatic underplating mostly underlies the wide margin at weak asymmetric conjugates, whereas the wide margin is mainly underlain by serpentinized mantle at strong asymmetric margins. Based on this conceptual template, we propose different natures for the COTs in the South Atlantic.

1. Introduction

In the last decades, a number of studies have shown that while some extensional margins follow the classical model of crustal and lithospheric break-up immediately followed by magmatic oceanic accretion (e.g., the Woodlark Basin; Taylor et al., 1999), others, the so-called magma-poor margins, exhibit large exposures of serpentinized mantle at a wide continent-ocean transition (COT). This transition is located between the oceanward end of the thinned continental crust and the first occurrence of magmatic oceanic crust. The West Iberia-Newfoundland conjugates and the ancient Tethys margins now exposed in the Alps have become archetypes for this margin style. In the former numerous drillings and geophysical surveys have been carried out, while the latter have been the focus of numerous field geology studies (e.g., Bayrakci et al., 2016; Boillot et al., 1987; Groupe-Galice, 1979; Lavier & Manatschal, 2006; Lemoine et al., 1986; Manatschal, 2004; Manatschal & Müntener., 2009; Masini et al., 2012; Mohn et al., 2010, 2012; Müntener et al., 2000; ODP Leg 173 Shipboard Scientific Party, 1998; Péron-Pinvidic et al., 2007; Reston et al., 1996; Sawyer et al., 1994; Tucholke & Sibuet, 2007; Tucholke et al., 2007; Welford et al., 2010; Whitmarsh & Miles, 1995; Whitmarsh et al., 1996, 1998). Whether or not the COT of margins consists of exhumed serpentinized mantle is relevant, among other reasons, because these areas may host intense serpentinite-based hydrothermal activity during continental break-up (Beard & Hopkinson, 2000; Klein et al., 2015). This involves production of hydrogen and methane at low temperature ranges that are within the limits of chemolithotropic life (Klein et al., 2015; Schrenk et al., 2013; Skelton et al., 2005), and the storage of water and element transfer from the mantle (e.g., Si, Mg, Ca), which may significantly impact magma-poor sedimentary environments (Pinto et al., 2017).

Typically, rifted margins were classified according to syn-rift magmatism. Magma-poor margins were thought to show scarce magmatism and exposed mantle at the COT, while magma-rich margins were characterized by an excess of magmatism. These two types of margins were considered to constitute end-members of a margin spectrum exhibiting variable degree of magmatism (e.g., Sawyer et al., 2007). Recent literature, however, classify many margins that do not show excess magmatism as magma-poor, i.e., place them toward one end of the margin spectrum. Some of these margins are the Gulf of Aden margin (Autin et al., 2010), the Goban Spur margin (Sibuet & Tucholke, 2013), the south Australian margin (Direen et al., 2007) and the South Atlantic Angola-Campos rift system and Santos and Espirito Santo basins (Pinto et al., 2017; Unternehr et al., 2010; Zalán et al., 2011; see also references to other margins in Reston, 2009). By analogy to the West Iberia-Newfoundland magma-poor conjugates, many of these margins have been interpreted to also have a COT consisting of exhumed and serpentinized mantle (e.g., Direen et al., 2013; Osmundsen & Ebbing, 2008; Peron-Pinvidic et al., 2017). However, drilling and detailed wide-angle seismic data at these COTs is still lacking to confirm this generalized interpretation (see also Eagles et al., 2015). The detailed nature of the COT at these margins may consist of exhumed mantle as in the archetypical West Iberia-Newfoundland margins, or of mainly magmatic products, perhaps underlain by serpentinized mantle, not yet forming a typical magmatic oceanic crust (see Figures 2a and 2b from Sawyer et al., 2007). Additionally, it is not clear whether exhumed mantle COTs also contain some 'hidden' magmatic products. For example, in the Iberia Abyssal plain sector of the West Iberia margin where the observational data set is one of the most complete up to date, the exhumed mantle may be underlain by a 2 km thick magmatic layer; an interpretation that also fits the geophysical data (Minshull, 2009; Russell & Whitmarsh, 2003; Sibuet et al., 2007). What appears to be clear is that magma-poor margins tend to extend at very slow velocities, within the realm of ultra-slow spreading velocities in oceanic ridges ($\leq$ 10 mm/yr half extension), where magmatism tends to be scarce.

Over the last decade, numerical modeling studies have become increasingly prevalent to understand the geodynamical processes involved in continental rifting (Beaumont & Ings, 2012; Nagel & Buck, 2004; Naliboff & Buiter, 2015). In particular, many authors have explored the relationship between the lower crustal strength and the tectonic evolution of margins with the goal of explaining the observed variability in the crustal asymmetry, faulting patterns and margin width (Bassi, 1995; Brune et al., 2017; Buck, 1991; Hopper & Buck, 1996; Huismans & Beaumont, 2014; Pérez-Gussinyé & Reston, 2001; Sharples et al., 2015; Svartman Dias et al., 2015; Wijns et al., 2005). These studies suggest that, for a strong lower crust, upper crustal deformation by faulting is highly coupled to mantle deformation by shear zones within the lower crust. These produce very effective crustal thinning, resulting in narrow symmetric margins characterized by large oceanward dipping faults that produce strong syn-rift subsidence (narrow rift mode, Buck, 1991; Type I, Huismans & Beaumont, 2011). However, for a weak lower crust, the deformation is distributed over a wide area, leading to the formation of wide symmetric margins, with small offset faults dipping both landward and oceanward and small syn-rift subsidence (wide rift mode, Buck, 1991; Type II, Huismans & Beaumont, 2011). For a lower crust of intermediate strength, the lower crust is strong enough to allow localization in a single active fault, although still weak enough to prevent rapid crustal break-up by faulting. In this case, localization of deformation in a single large fault leads to asymmetric uplift of the mantle, heating and weakening the hangingwall of the large active fault, where the next fault will form. This leads to the emergence of an oceanward younging and dipping fault array which is sequential in time, and which generates a marked margin asymmetry (Brune et al., 2014, 2017; Ranero & Pérez-Gussinyé, 2010). In this study we use numerical modeling to analyze whether these extensional modes (i.e., narrow, wide and sequential faulting) can also be related to COT types. We distinguish between COTs where serpentinized mantle is dominant at the top basement and COTs that are predominantly magmatic.

In particular, our contribution focuses on the role of lower crustal strength in determining the rate of mantle upwelling versus the rate of crustal embrittlement. This, in turn, controls the relative timing of the onsets of melting and serpentinization during extension and, hence, the nature and extent of the COT (Minshull et al., 2001; Pérez-Gussinyé & Reston, 2001; Pérez-Gussinyé et al., 2006). The concept that the relative timings of melting and serpentinization may control the nature of the COT is based on the notion that serpentinized mantle may act as a barrier for melt migration. In this work we assume that once melts are generated, they quickly move to the area of maximum extension beneath the crust (Gudmundsson, 1990, 2011). When this

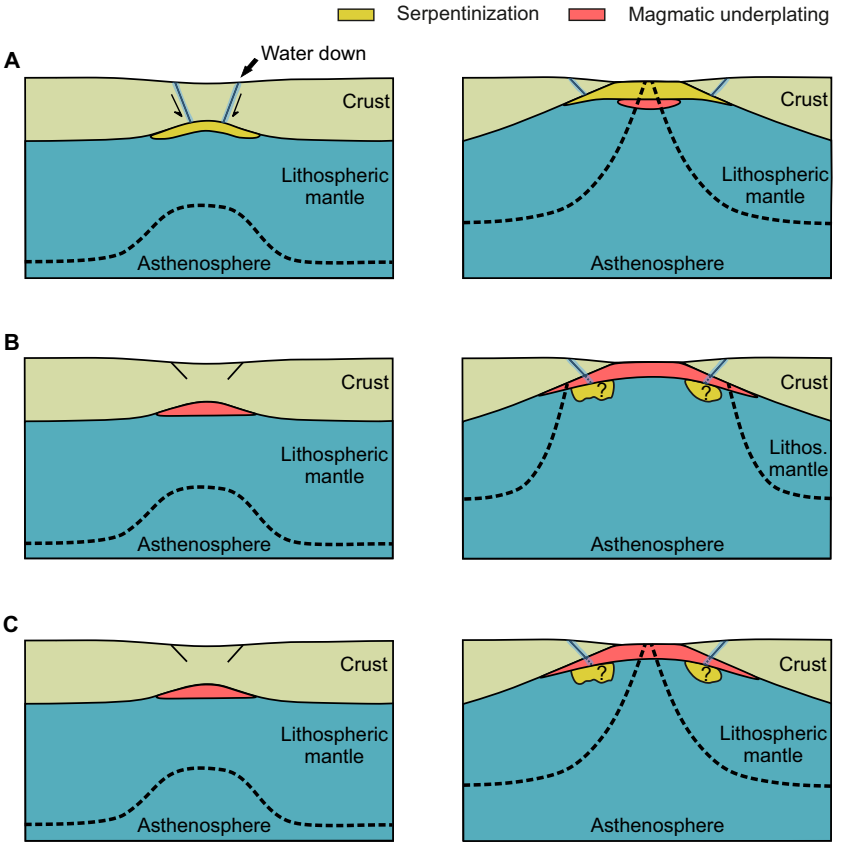

Figure 1. Cartoons showing three break-up styles of magma-poor continental rifting. (a) Brittle lower crust allows the formation of crustal-scale faults that act as conduits for the water, which reaches the mantle and serpentinize it before melting starts. The crust breaks-up before the lithosphere mantle and the resulting COT shows exhumed and serpentinized mantle, underlain by magmatic underplating. (b) Ductile lower crust inhibits the formation of crustal-scale faults until later in rifting history, hence melting starts before serpentinization. The mantle lithosphere breaks-up before the crust, resulting in a magmatic dominated COT, perhaps underlain by serpentinized mantle. (c) Ductile lower crust inhibits the formation of crustal-scale faults until later in rifting history. The crust breaks-up before the lithosphere mantle and a magmatic dominated COT results, below which may be serpentinites. No exposed mantle is observed in cases B and C, regardless of the relative timing between the crust and lithosphere mantle rupture.

area has been already occupied by serpentinized mantle, two factors may hinder the ascent of melt to upper levels within the crust and/or their extrusion (Figure 1a). First, serpentinized mantle may act as an 'impermeable' barrier to melt transport by porous flow. We base this assumption on the fact that, in subduction zones, serpentinites have been proposed to be impermeable in the direction perpendicular to shearing at the subducting plate interface (Katayama et al., 2009; Kawano et al., 2011). This suggests that, in extensional environments, a layer of serpentinized mantle may also act as a barrier to vertical melt migration. Second, if melt is intruding by diking in the brittle regime, then nondilatant brittle deformation of serpentinite (Escartin et al., 1997) may act as an additional stress barrier that the dike has to overcome. Alternatively, other magma/serpentine interactions could lead to serpentinites being a natural barrier to dike propagation. For example, if the hot dike magma induces rapid devolatilization of serpentine at the serpentine contact, this large pulse of volatiles could induce fracture along the serpentinized mantle interface that favors the dike propagating alongside, rather than into the region of serpentinized mantle. Furthermore, serpentine devolatilization is strongly endothermic, thus favoring more rapid dike cooling/freezing. All these scenarios do not exclude the possibility that melt eventually intrudes the serpentinite layer, but rather stress that the presence of serpentinite can hinder the intrusion of melt through serpentine to reach the top basement. Hence, when serpentinization has occurred prior to melting, the COT could tend to appear as mainly serpentinized mantle at the surface, with melts being mostly underplated or intruded into the serpentinite layer, and only a small volume of extruded melt products (Figure 1a).

The necessary conditions for mantle to be exhumed at the COT have been considered in previous studies of numerical modeling. Some authors concluded that mantle is exhumed at the COT when crustal break-up occurs before lithospheric break-up (e.g., Type 1 margins; Huismans & Beaumont, 2011; Figure 1a). However, these models do not include the generation of magma nor of serpentinization during continental rifting, which is crucial for understanding the nature of the COT. We show that in extensional margins where melting begins relatively early in the rifting process, irrespective of whether the lithosphere (Figure 1b) or the crust 'breaks' first (Figure 1c), melt ascends to underplate the crust prior to serpentinization, thus moving regions of potential serpentinization to deeper and hotter levels in the mantle, where serpentinization is less likely. Hence, these margins should be characterized by more magmatism and much less serpentinization, generating an abrupt transition to magmatic oceanic crust with no exposed mantle (Figures 1b and 1c).

In this work, we include melting and the serpentinization of the mantle in numerical models to assess the amount, timing and distribution of melts and serpentinized mantle during continental rifting. Our models suggest that extension at ultra-slow velocities does not necessarily lead to mantle exhumation at the COT of magma-poor margins and that mantle exhumation is strongly dependent on lower crustal strength. Additionally, we use numerical modeling as a further tool to help interpret and understand the processes leading to COT formation. We qualitatively compare the tectonic style of our model results to 3 interpreted seismic profiles in the central South Atlantic segment (Figure 2). We are not aiming to reproduce all the features of the South Atlantic margins to validate our model results, but instead to use both numerical and seismic profiles for comparison between the first order characteristic of the margins tectonic styles, including margins widths, faulting patterns, and crustal deformation, in order to make predictions on the nature of the COTs along the profiles. Definite observations are still lacking concerning the nature of the COT in this margin sector due to the relative lack of wide-angle seismic data and drilling. To date, only a refraction survey in the Santos basin has been published (Evain et al., 2015); this shows a magmatic COT. Below we will briefly summarize the tectonic structure of the margins in our study area and the different interpretations that have been given to the COTs at these margins in previous studies.

2. Study Area

Opening of the central South Atlantic segment propagated northward from the Rio Grande Fracture Zone to the Ascension Fracture Zone (Blaich et al., 2011; Eagles, 2007; Pérez-Díaz & Eagles, 2014) and lasted about 30 Myr, from the Late Jurassic/Early Cretaceous to the Aptian (Heine et al., 2013). The study area encompasses three representative conjugate margins: Camamu/South Gabon, Campos/North Kwanza and North Santos/South Kwanza (Figure 2). There is still some debate on the timing and location of break-up because it occurred during the Cretaceous Magnetic Quiet period (Bird & Hall, 2016). The location and extent of the continent-ocean transition (COT) is also debated because the present interpretations are based only on multichannel seismic data, except for the section we use in the Santos basin.

Figure 2 shows the landward limit of the oceanic crust (LaLOC) from Heine et al. (2013). This limit separates homogenous oceanic crust from an area that could include some transitional crust between the continental and oceanic domains. In the two southern sectors of our study area, the LaLOC is at most 30–40 km oceanward from the COB defined by Blaich et al. (2011) while in the northern area is almost coincident. This difference arises partly because the LaLOC allows the inclusion of transitional crust and the COB by Blaich et al. (2010, 2011) represents the oceanward limit of the continental crust. The LaLOC in Figure 2 is used to give a picture of the first-order variation of the margin width in the whole study area. However, we use more regional studies in the areas of the seismic sections for our seismic interpretations, e.g., Blaich et al. (2011) and Lentini et al. (2010) in the two southern sectors, and Blaich et al. (2010) in the northern sector. Despite these various interpretations on the continental margin width, they all exhibit a very marked change in polarity from North to South (Figure 2d). The Brazilian and African margins exhibit opposite tendencies, with the former increasing in width toward the South and the latter decreasing. Below, we briefly describe interpretations of seismic lines in these key sectors, which show a change in the style of extension from the Camamu/Gabon sector, where the margins developed close to the San Francisco craton, to the Campos/North Kwanza and North Santos/South Kwanza sectors, where the margins developed close to the Ribeira fold belt.

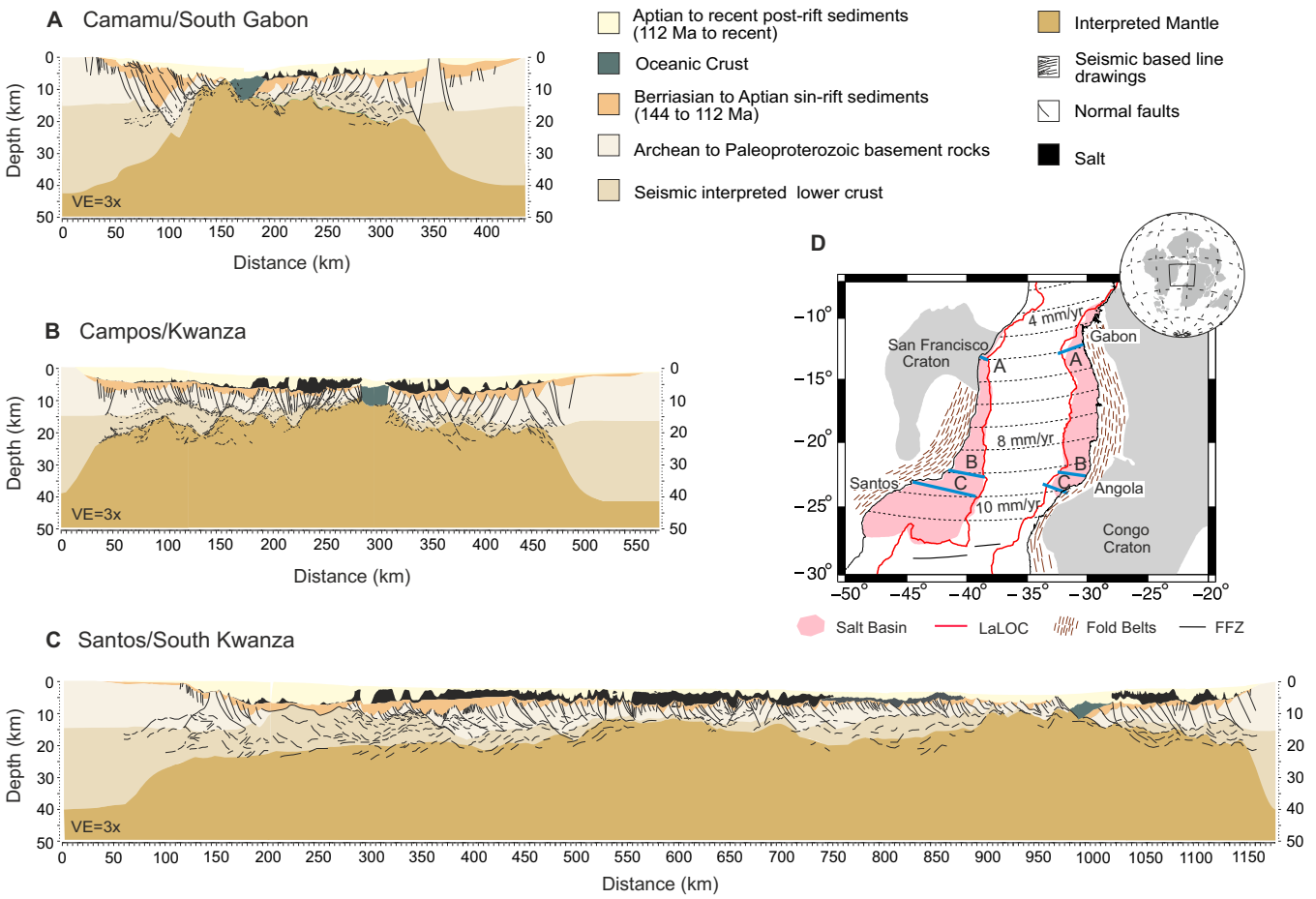

Figure 2. Geological interpretation of central South Atlantic conjugate margins. (a) Interpretation of seismic line in Camamu/South Gabon. Asymmetric narrow-wide margin configuration, with the Brazilian margin thinning abruptly over $<$ 100 km and the African conjugate gradually thinning over 200 km. Note large faults dip mostly oceanward and exhibit large syn-riftt subsidence. (b) Interpretation of seismic line in Campos/North Kwanza. Symmetric wide domains with a $\sim$ 500 km conjugate width. Note small faults, dipping ocean- and landward, exhibiting small syn-rift subsidence. (c) Interpretation of seismic line in North Santos/South Kwanza. Asymmetric margins with a 950 km margin width in North Santos and a 200 km width in South Kwanza. Note small faults, dipping ocean- and landward, and small syn-rift subsidence. Crustal thicknesses offshore were constrained by 2-D gravity modeling and onshore by receiver function and tomographic maps of Assumpção et al. (2013). In the specific case of the Santos Basin, the interpretation was also supported by the wide-angle refraction seismic of Evain et al. (2015). (d) Plate reconstruction of the South Atlantic (Africa is kept fixed) (adapted from Heine et al., 2013) with the locations of the interpreted seismic sections. The LaLOC is the landward limit of the oceanic crust from Heine et al. (2013). From North to South the degree of asymmetry and the full-extension velocity increases. The rheology changes from craton to fold belt as we move southward. FFZ is Florianópolis Fracture Zone from Pérez-Díaz and Eagles (2014). V.E. Vertical Exaggeration.

2.1. Interpretation of Seismic Lines

The locations of the interpreted seismic lines of the South Atlantic central segment used in this study are shown in Figure 2. The corresponding seismic lines are proprietary data of ION-GXT and have been already published (Blaich et al., 2010; Ferreira et al., 2009; Kumar et al., 2013; Zalan et al., 2011). Any interpretation of multichannel seismic data is a subjective process, especially when the seismic image is not sharp, as is sometimes the case under some areas in the salt basins of the Campos and Santos. In this study we present interpretations of the first-order characteristics that define margin tectonic style where there is more agreement. These include the width of the continental margin, the asymmetry of the conjugates, the fault associated subsidence and the faulting pattern. We describe the latter based on the offset, dip direction and spatial distribution of faults. For example, we examine whether the shelf break exhibits large faults with accompanying abrupt syn-rift subsidence, or whether along the hyperextended sector of the seismic sections, where crustal thickness is less than 15 km, faults dip predominantly in one direction or randomly. These first-order faulting patterns are typically well recognized in seismic sections. Crustal thicknesses

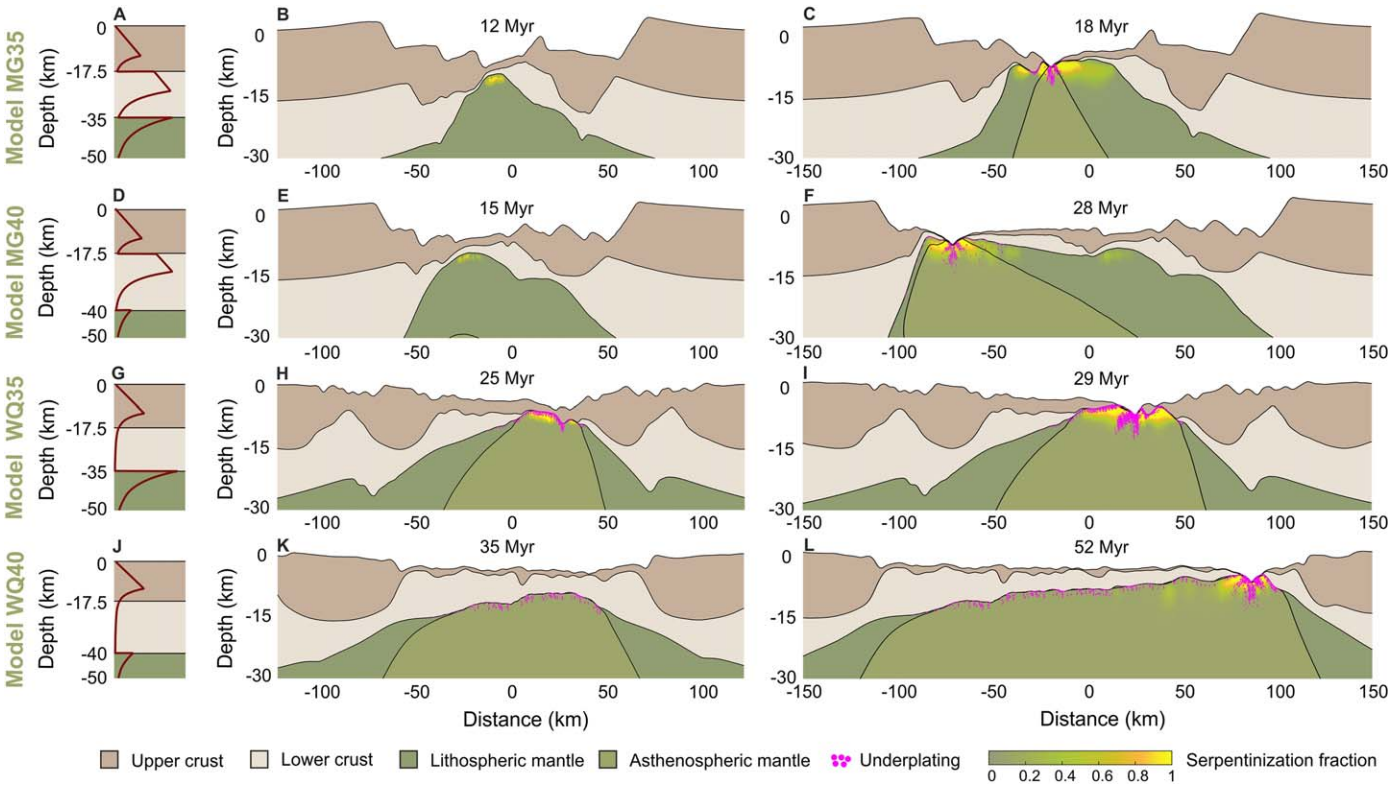

Figure 3. Initial strength envelope (A, D, G, J), intermediate snapshot (B, E, H, K) and break-up snapshot (C, F, I, L) of the MG35, MG40, WQ35 and WQ40 numerical models, respectively. Lower crusts are of mafic granulite (MG) or wet quartzite (WQ) and crustal thicknesses are thin (35) or thick (40). Snapshots show rheological layers, serpentinization with a color scale and underplating in pink color (see Legend). Note that the snapshots show the most representative times for each model. A movie with the evolution of each model can be found in the supporting information.

offshore were constrained by 2-D gravity modeling and onshore by receiver function and tomographic maps of Assumpção et al. (2013). In the specific case of the Santos Basin, the interpretation is also supported by wide-angle refraction data of Evain et al. (2015). We qualitatively compare these interpreted first-order margin characteristics with those observed in numerical models to make predictions about the COT nature along the interpreted sections.

Our interpretations in the Santos-South Kwanza and Campos-Kwanza lines are very similar to those published by Kumar et al. (2013; their Figures 5 and 9). In the Camamu-Gabon sector our interpretation is in accord with that published by Blaich et al. (2011; their Figure 3). Although we could have simply used the previous interpretations from the literature, we felt the need to provide an integrated view of the conjugated margins in terms of asymmetry, thinning profile, margin width and faulting pattern. Such integrated view was only possible by revisiting the seismic lines, which is shown below.

At basin scale the seismic lines show significant differences in the pattern of faulting distribution and depocentre depths. We assume that the present day crustal thicknesses estimated onshore are unthinned continental crusts. Therefore, we define the length of the margins from the unthinned continental crust to the COB. In the North, the Camamu/Southern Gabon margin pair is asymmetric, with the short conjugate margin on the Brazilian side and long one on the Gabon side (Figure 2a). Here the proximal zones are subdivided into large blocks, bounded by faults with offsets between 7 and 8 km (Araújo et al., 2015). These faults control deep depocentres, probably related to a stage of large syn-tectonic subsidence. Faults dip mainly oceanward on both margins. Another important characteristic is the crustal thinning of the crust, changing from a 40 km thickness to 10 km within a short distance (20 km) on the Brazilian side. In the Gabon side, crustal thinning is much smoother, so that the margin is much wider than on the Brazilian side. This configuration defines a marked asymmetry with a total length of 430 km. Our interpretation is quite similar to that recorded by Blaich et al. (2011). The occurrence of strong asymmetry, accompanied by oceanward dipping faults exhibiting large offsets, suggests deformation of an intermediate lower crustal strength

by sequential faulting mode, leading to the formation of a wide hyper-extended margin and a narrow conjugate (Brune et al., 2014, 2017; Ranero & Pérez-Gussinyé, 2010).

Southward, the conjugate margin pair of the Campos/Kwanza basins developed on the Neoproterozoic Ribeira/Kaoko Mobile Belt that extends over more than 500 km (Figure 2b). In terms of length, this sector is much wider, reaching a maximum length of 560 km. In both margins there are segments of typically hyper-extended crust (thickness $<$ 10 km). These widths are $\sim$ 250 km in the Campos basin and 140 km in Kwanza basin. Faults dip both landward and basinward, only in the distal parts of the margins do they systematically dip oceanward. These faults show small offsets (2.5 km), defining depocentres of similar depth values. This large width of the conjugate margins, in combination with smooth crustal thinning profile and the absence of large fault offsets suggest deformation in wide rift mode or Type II margins (Buck, 1991; Huismans & Beaumont, 2011), with a predominance of ductile deformation during extension.

To the South, the margins of North Santos/South Kwanza show thinning that is extremely large and asymmetric between the conjugate margins (Figure 2c). The Northern section of the Santos Basin also developed on the Ribeira/Kaoko fold belt but in a region with crust thicker than 40 km. Here the main characteristic is a very wide margin in the Brazilian side- over $\sim$ 800 km- while the conjugate South Kwanza margin is much shorter ($\sim$ 200 km). The gentle crustal thinning profile from the Brazilian platform to the hyperextended sector, the presence of divergent horst and grabens, with typically small offsets, and the large width of the conjugate margin all suggest the importance of ductile lower crustal deformation during extension. Note that the opening of this margin sector evolves with a 3-D structural heterogeneity and that the profile we show is oblique to the average opening direction, such that the Brazilian margin width in the extension direction may be 30% shorter.

2.2. Previous Interpretations of the COT in Our Study Area

The nature of the COT in our study area has been a topic of much debate in the recent years. Along the Camamu and Espirito Santo margins, Blaich et al. (2010, 2011) interpret the COT to be rotated fault blocks and wedge-shaped syn-rift sediments, where the thinned continental crust could be likely intruded by mafic material. Peron-Pinvidic et al. (2017) interpret the COTs of the Gabon and Kwanza as exhumed mantle which can be variously serpentinized. Mohriak et al. (2012) characterize the Espirito Santos-Kwanza margins with a magmatic COT. Unternehr et al. (2010) apply the conceptual model of Lavier and Manatschal (2006) to the seismic profiles of Campos and Angola in order to interpret the COT as exhumed mantle. This interpretation is also made by Zalán et al. (2011), who state that a serpentinized exhumed mantle transition can be mapped from Espirito Santo to Santos basins. However, Mohriak et al. (2008), Aslanian et al. (2009) and Kumar et al. (2013) suggest that extension in this area may have been partly accomplished by volcanic extrusions and intrusions and do not find evidence of exhumed mantle (except maybe along the Florianopolis fracture zone). Finally, wide-angle seismic data indicate an abrupt transition to normal oceanic crust in the Santos Basin (Evain et al., 2015).

3. Methods

We model extension of a rheologically layered visco-elasto-plastic lithosphere using a 2-D numerical code based on the Finite Element Method MILAMIN solvers (Dabrowski et al., 2008). The code uses a Lagrangian formulation to solve the conservation equations of mass, momentum and energy for an incompressible Stokes flow (see supporting information; Lu et al., 2011). Strain softening is included in the plastic and viscous deformation to localize deformation into shear bands that mimic faults in nature (see supporting information; Bos & Spiers, 2002; Buck & Lavier, 2001; Buck & Poliakov, 1998; De Bresser et al., 2001; Huismans & Beaumont, 2002; Lavier et al., 1999; Malvern, 1969; Précigout & Gueydan, 2009).

Decompression melting occurs where the mantle temperature exceeds the dry solidus (see supporting information Figures S1A and S1B). Melt generation is calculated at each time step based on the formulation of Morgan (2001), and the total amount of melt is located at the base of the crust forming a dike (Ito et al., 1996, see Figure 3 and section "Melt productivity and emplacement" in supporting information; Lavecchia et al., 2017; Schmeling, 2010; Simon et al., 2009). The production of melt depletes the mantle source and decreases its density (see section "Thermal and rheological profiles" in supporting information; Armitage et al., 2013). We assume that no melt is retained in the mantle and that after 4% of depletion the mantle

source has removed all the water, leading to a change in rheology from wet to dry olivine. This dehydration effect on the rheology will strength the mantle source.

In nature, as melt is produced, it ascends and either underplates, intrudes the crust or is extruded (Cannat et al., 2009). Underplating and intrusion can occur in the form of dikes and sills (Mathieu et al., 2008). For our numerical models we choose to accumulate all the melt produced at each time step in a column with a width equal to the full spreading velocity multiplied by the model time step, and a vertical thickness equal to the volume of produced melt divided by the width. We refer to the vertical thickness of the melt column as the magmatic crustal thickness by its analogy to the magmatic crustal thickness that would be produced in an oceanic ridge (Dick et al., 2003). Because the melt is placed at each time step in a new column, we refer to this column as dike. At each time step the new `dike` is positioned below the Moho in the location of maximum extension. The increasing number of dikes during rifting accumulates beneath the Moho and form what we call magmatic underplating (Thybo & Artemieva, 2013).

We allow serpentinization to occur when three conditions are met: the crust is entirely brittle, faults are active and the mantle is within the temperature range for serpentinization (~100 - 450°C). The first two criteria assume that the main conduits of water to serpentinize the mantle are active crustal-scale faults, as described in Pérez-Gussinyé and Reston (2001) and Bayrakci et al. (2016). The rate and extent of serpentinization is calculated with a dependence on temperature given by experimental data (Emmanuel & Berkowitz, 2006; see supporting information Figure S1C). The transformation of olivine into serpentinites releases heat to the surrounding rock as $Q=-H\frac{\partial \rho_m}{\partial t}$ where ρ_m is the mass of forsterite per unit volume, t is the time and H is the heat reaction per unit mass of forsterite. In study we assume a temperature raise $300^{\circ}C$ for complete serpentinization. The viscosity of the serpentinized mantle decreases with the raise in temperature, which in turn reduces its ductile strength, and the density is the same as the mantle density. Since our numerical code is incompressible, we neglect the volume increase that results from serpentinization. This effect would promote strain localization along serpentinized fault planes (Iyer, 2007), which may help the formation of detachment faults. To define which faults are active we use a parameter that estimates how large the strain rate is within the fault in comparison to the maximum and minimum strain rates in the model domain. The exact definition of this parameter and how it influences our estimations of serpentinization is described below.

In nature, the production of serpentinized mantle depends on many factors, including the permeability and porosity of the active faults that control the access of water to the mantle (Emmanuel & Berkowitz, 2006; Macdonald & Fyfe, 1985). The numerical threshold that defines active faults cutting through the crust is subject of discussion. Here, we consider active the faults with larger strain rates than a threshold value $\dot{\varepsilon}_{th}$, which is calculated from the maximum and minimum strain rates ($\dot{\varepsilon}_{\max}$ and $\dot{\varepsilon}_{\min}$) along the model domain $\dot{\varepsilon}_{th}=f\cdot(\dot{\varepsilon}_{\max}-\dot{\varepsilon}_{\min})+\dot{\varepsilon}_{\min}$, where f is an arbitrary factor ranging from 0 to 1. We ran sensitivity tests to the f factor by varying its value from 0.001 to 0.5 (corresponding to the 0.1% and the 50% of the strain rate variation, respectively) with crustal thickness of 35 km, half-extension velocity of 3 mm/yr and two different lower crustal rheologies: mafic granulite and wet quartzite (supporting information Figure S2). The models with a larger f resulted in a slight delay of the onset of serpentinization (~ 0.1 to 0.4 Myr, for mafic granulite and wet quartzite, respectively) and less amount of serpentinized mantle. The difference in the parameter influences mainly the depth at which water is simulated to reach the mantle, and therefore the depth of the serpentinized zone, which changes about 5 km. Consequently, the degree of serpentinization is also affected, obtaining larger zones of 100% serpentinized mantle for the lower parameter. From wide-angle seismic refraction studies in the Iberia Abyssal Plain, highly serpentinized mantle up to 100% has been estimated in the COT, which decreases with depth (Chian et al., 1999), consistent with results from ODP drilling (Sawyer et al., 1994). Despite the small differences, the general outcomes for the nature and composition of the COTs hold after varying this numerical threshold within a reasonable range (supporting information Figure S2). The threshold parameter value assumed for this study is 0.15. Although this modeling parameter is not well constrained, we consider that our assumption for crust-cutting active faults better approximates the locations for generation of serpentinization in comparison to the condition with a merely brittle crust.

3.1. Model Setup

The 2-D model domain is 400 km wide by 400 km deep. The boundary conditions prescribed at the lateral and bottom boundaries are tangential free slip, with half-extension rate at the sides and full-extension rate

at the bottom to preserve the conservation of mass. This approach upwells the asthenospheric bottom as pure shear. Free surface is applied to the top boundary (Andrés-Martínez et al., 2015; Kaus et al., 2010). We run model simulations by applying different half-extension velocities within the ultra-slow range (3, 5 and 10 mm/yr), as Heine et al. (2013) suggested for this area (Figure 2d), to explore the implications of increasing the velocity on the COT nature.

Table S1 shows the rheological parameters used for modeling (Gleason & Tullis, 1995; Hirth & Kohlstedt, 2003; Ranalli & Murphy, 1987; Wilks & Carter, 1990): a wet olivine asthenosphere, dry olivine lithospheric mantle and wet quartzite upper crust (see section "Thermal and rheological profiles" in supporting information; Currie & Hyndman, 2006; Hirth & Kohlstedt, 1996; Morgan, 1997; Ranalli, 1995; Rüpke et al., 2006). To make simple and comparable simulations, we only change the strength of the lower crust between two rheologies: strong mafic granulite and weak wet quartzite. These rheologies are not meant to simulate the real composition of the lower crust, but rather are used as end-member strengths for the lower crust. When comparing to our study area, it must be kept in mind that, presently, there is not enough data on the onshore lithospheric structure that could give us detailed information on the rheology at the time of rifting. So we make informed guesses and compare the tectonic style observed in our seismic lines with the model results of the end-member rheologies. In the North of our study area, the rifting developed close to or at the San Francisco craton, so we assume that the lower crustal rheology was likely to be strong there. Continent-wide tomography results and high Te underneath the San Francisco craton indicate a thicker and colder lithosphere under this area (Feng et al., 2007; Pérez-Gussinyé et al., 2007, 2009). The lower crust and lithosphere under cratons is conventionally assumed to be strong (see strength envelopes in Burov, 2011), thus we compare our profile to the strong-end member case, mafic-granulite.

Toward the South, the rift develops on top of the Ribeira-Kaoko fold belt, the rocks are much younger and dominantly composed by gneisses and metasedimentary rocks metamorphosed from upper greenschist to amphibolite and few regions with granulites (Heilbron et al., 2008). The gentle continental slope and crustal tapering, in combination with the large width of these margins indicates that the lower crust must have been weak during rifting. This weakness may have been in part the result of the thermal influence of the Tristan da Cunha Plume during the onset of rifting (136 Ma). We use our weak end-member rheology to compare with the tectocnic style in this area. In addition, we change lower crustal strength by increasing crustal thickness from 35 km to 40 km, which are the crustal thicknesses observed in our study area (Assumpcão et al., 2013).

4. Results

Based on the relative onsets of serpentinization and melting, we describe the type of COT that would be expected for the weak and strong end-member strengths and various extensional velocities, i.e., 3, 5 and 10 mm/yr, used in this study. Similar to previous numerical models, our results show margin tectonic styles ranging from narrow to wide and from symmetric to asymmetric style as the lower crustal strength changes (Figure 3; e.g., Bassi et al., 1993; Brune et al., 2017; Buiter et al., 2008; Dunbar & Sawyer, 1989; Huismans & Beaumont, 2014; Naliboff & Buiter, 2015; Svartman Dias et al., 2015; Tetreault & Buiter, 2017). We decrease the lower crustal strength by changing the lower crustal rheology from strong mafic granulite to weak wet quartzite and by varying the crustal thickness from 35 to 40 km. For a given crustal thickness, the strong lower crust model always leads to narrower margins than the weak case (Figure 3), as already described in numerous publications (e.g., Bassi, 1991; Buck, 1991; Huismans & Beaumont, 2011). For any given lower crustal rheology, the conjugate margins become more asymmetric as the crustal thickness increases (Figure 3). Below we describe how the lower crustal strength affects the tectonic style and the production and timing of melting and serpentinization in our model runs of 3 mm/yr half-extension velocity (Figure 3).

For the strongest and thinnest lower crust case (Model MG35; Figures 3a–3c and supporting information Movie S1), the low thermal gradients that prevail during rifting result in strong localization of the deformation into large fault offsets, causing effective crustal thinning and embrittlement of the lower crust. At 11 Myr crustal faults that reach the mantle and act as conduits for water, allow serpentinization to start beneath ~3–4 km thick crust, where the mantle is at temperatures suitable for serpentinization (Figure 3b and supporting information Movie S1). At this time the thermal gradient is still too low for the mantle to melt (Figures 3b and 4a). The narrow extensional mode (as described by Buck, 1991) dominates rifting and

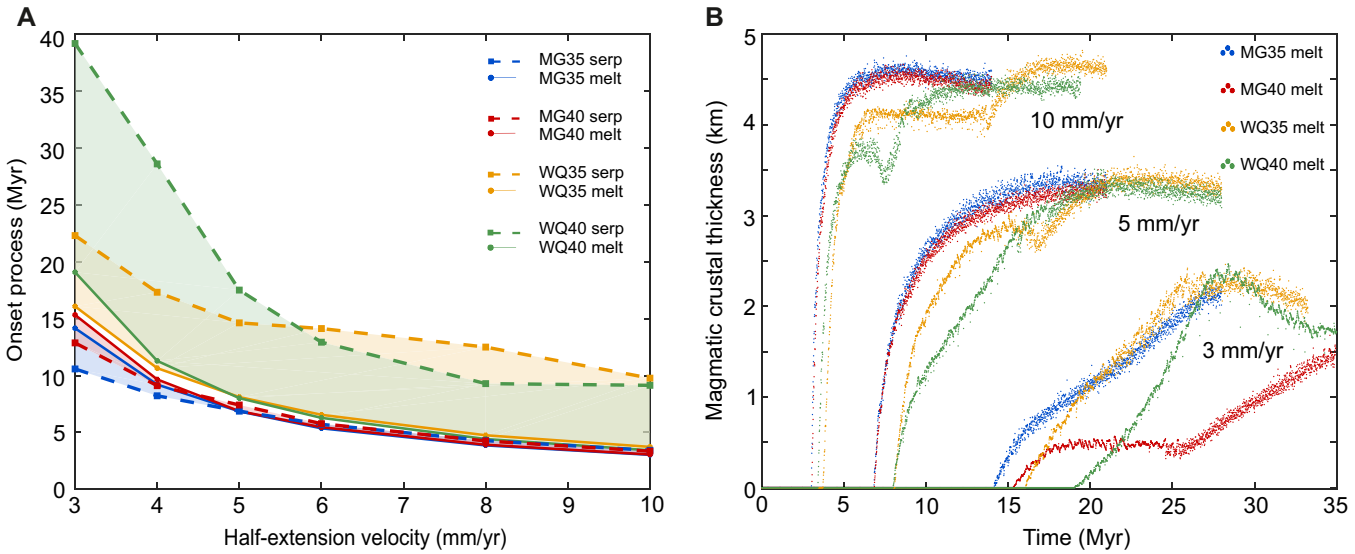

Figure 4. Numerical model results for the onset of melting and serpentinization and for the predicted magmatic crustal thickness. Models with mafic granulite lower crust are shown in blue and red colors for the 35 and 40 km thickness cases, respectively. Models with wet quartzite lower crust are shown in yellow and green colors for the 35 and 40 km thickness cases, respectively. (a) Melting and serpentinization onsets during the evolution of the numerical models, where models with half-extension velocities of 4, 6 and 8 mm/yr have been included to refine the transition between velocities. Solid and dashed lines link the onsets of melting and serpentinization, respectively, for the same lower crustal rheology and different extension velocities. (b) Predicted magmatic crustal thickness evolution over time.

leads to symmetric narrow conjugate margins. An earlier onset of serpentinization than that of melting results in a COT dominated by exhumed serpentinized lithospheric mantle at the seafloor, underplated by a thin magmatic layer (Figure 3c).

An increase in the lower crustal thickness implies a weakening at the bottom of the crust, so that the level of crust-mantle coupling decreases in comparison to the previous case (see strength envelopes in Figures 3a and 3d). This promotes a switch from the initial narrow deformation mode to a sequential faulting mode after 10 Myr of extension (Model MG40, Figures 3e and 3f; supporting information Movie S2). The latter mode occurs where deformation localizes in a single active fault and the lower crust is weak enough to flow to the fault tip. This inhibits crustal break-up by faulting and promotes the generation of a sequence of active faults that laterally migrate the rift center and dip oceanward, resulting in asymmetric conjugate margins (see Brune et al., 2014; Ranero & Pérez-Gussinyé, 2010). As sequential faulting progresses, serpentinization starts before melting (at 13 Myr; Figure 3e and supporting information Movie S2). Serpentinization does not occur as a consequence of the water moving down through the main active oceanward fault because the ductile lower crust flow does not allow the fault to reach the mantle. Instead, serpentinization is generated as the water downflows through the much less prominent faults dipping landward. These are located in the immediate footwall of the active fault, where the crust is thinner than 4 km (Figure 3e and supporting information Movie S2). We observe in our tests that serpentinization occurs in the footwall of the main active fault, which differs from the interpretation of Bayrakci et al. (2016) who suggested that, during the sequential faulting mode in the Deep Galicia margin, antithetic faults to the main active fault developed and acted as water conduits, which would explain the apparent focus of serpentinization underneath the hanging walls of normal faults in the margin. However, the sequential faulting mode is characterized by the development of a lower crustal flow that partly decouples crust and mantle at the tip of the fault, heating up this zone and inhibiting the formation of faults, in the hanging wall, that reach the mantle (Brune et al., 2014). Pinto et al. (2015) highlighted the difficulty in determining the pathways for the seawater migration into the mantle and proposed two options: through synthetic and antithetic normal faults in the hanging wall of a detachment fault or along the detachment itself, showing a more serpentinized footwall. Both types of water down flow would, however, produce very similar serpentinization profiles. Eventually, conductive cooling embrittles the lower crust and allows crustal break-up to occur ~9 Myr later than in the previous case with a thinner crust. The spatial extent of serpentinization beneath the thinned crust is much larger in the wide margin (20–30 km) than in the narrow one. Very little underplated magma is observed

beneath the crust on both margin sides (< 0.5 km; Figures 3f and 4b and supporting information Movie S2). The COT is characterized by exhumed serpentinized mantle at the seafloor, intruded and underplated by very little amounts of frozen magma (< 1.5 km; Figures 3f and 4b).

For the weakest and thinnest lower crust (Model WQ35, Figures 3g–3i), the increased degree of crust-mantle decoupling compared to the two previous cases, results in distributed faulting over a wide zone, with uniform crustal and lithosphere mantle thinning (i.e., wide rift mode, Buck, 1991) (from 0 to 11 Myr; Movie S3). The weak lower crustal flow inhibits the formation of crustal-scale faults, which delays the onset of serpentinization to 23 Myr, i.e., 6 Myr after the onset of melting (Figures 3h and 4a; supporting information Movie S3). Break-up leads to conjugate margins that are mostly symmetric, where the slightly wider margin results from a last stage of sequential faulting, as shown in Movie S3. Mantle serpentinization starts after melting, therefore the serpentinized zone is generated beneath the already frozen magma underplating the crust. We consider the COT to be a magma-dominated domain where magma products can be found at the sea-floor, and may be underlain by serpentinized mantle (Figure 3i).

For the same weak rheology and thicker lower crust (Model WQ40; Figures 3j–3l) extension starts in core complex mode (Buck, 1991; Tirel et al., 2008), localizing deformation in upper crustal detachment faults, whereas the lower crust and lithosphere mantle accommodates deformation over a wide region (from 0 to 12 Myr; Movie S4). As extension continues, the deformation changes to wide mode until 32 Myr. Later cooling kicks in leading to localization of deformation where the crust is the thickest, as the cooled mantle in the thinned region is stronger (e.g., Bassi et al., 1993), and switches to sequential faulting mode at 34 Myr. Melting starts at 19 Myr whereas serpentinization starts 21 Myr after melting (Figure 4a and supporting information Movie S4). Sequential faulting in the last stages of extension leads to the formation of two asymmetric margins, where the hyper-extended wide margin is underplated by magma along much of its length ∼150 km (Figure 3l). This contrasts with the asymmetric model of a strong lower crust (Figure 3f) in which the wide margin is underplated by serpentinized mantle (compare Figures 3e and 3f with Figures 3k and 3l). The COT is magma dominated, with magmatic products at the seafloor, perhaps underlain by some serpentinized mantle (Figure 3l).

To obtain extremely wide and symmetric margins (e.g., Type II from Huismans & Beaumont, 2011 and Brune et al., 2017), we have to decrease the upper and lower crustal strengths from that in our standard models (see supporting information Figure S3 and Table S1 for rheological parameters). This very weak crustal model starts with a high degree of crust-mantle decoupling, which promotes distributed faulting in a wide mode that dominates the rift evolution and eventually leads to symmetric wide conjugate margins underplated by magma and a magmatic dominated COT.

When extension velocity is higher (5 and 10 mm/yr) all cases undergo melting prior to serpentinization, independently of the lower crustal rheology (Figure 4a and supporting information Figure S4). This is because higher velocities result in faster mantle uplift, which allows melting to start before serpentinization. At 5 mm/yr and for strong lower crusts, serpentinization takes place short after melting (< 1 Myr) due to the rapid embrittlement of the crust, most likely resulting in a narrow COT with both exhumed serpentinized mantle and magmatic products. For weak lower crusts, serpentinization occurs much later than melting in all cases, suggesting that for weak rheologies COTs will be dominated by magma without exhumation of lithospheric mantle for any ultra-slow extension velocity.

5. Discussion

5.1. Dependence of Melting on Lower Crustal Strength

It is well known that during oceanic spreading and continental rifting melting mainly depends on mantle temperature, composition and extension velocity (Armitage et al., 2009; Bown & White, 1995; Jokat et al., 2003; Morgan, 1987; Sotin & Parmentier, 1989; White et al., 2001). Figure 4a shows the dependence of mantle melting on lower crustal strength for ultra-slow extension velocities (≤ 10 mm/yr half-extension) which predominate in magma-poor environments. This dependence is most obvious for the cases with the lowest velocities tested here, 3 and 4 mm/yr, and determines the nature and extent of the COT. For 3 mm/yr, the strong and thin mafic granulite lower crust melting starts at 14 Myr, whereas for the thick and weak wet quartzite it starts at 19 Myr (Figures 4a and 4b and supporting information Movie S5). Despite being

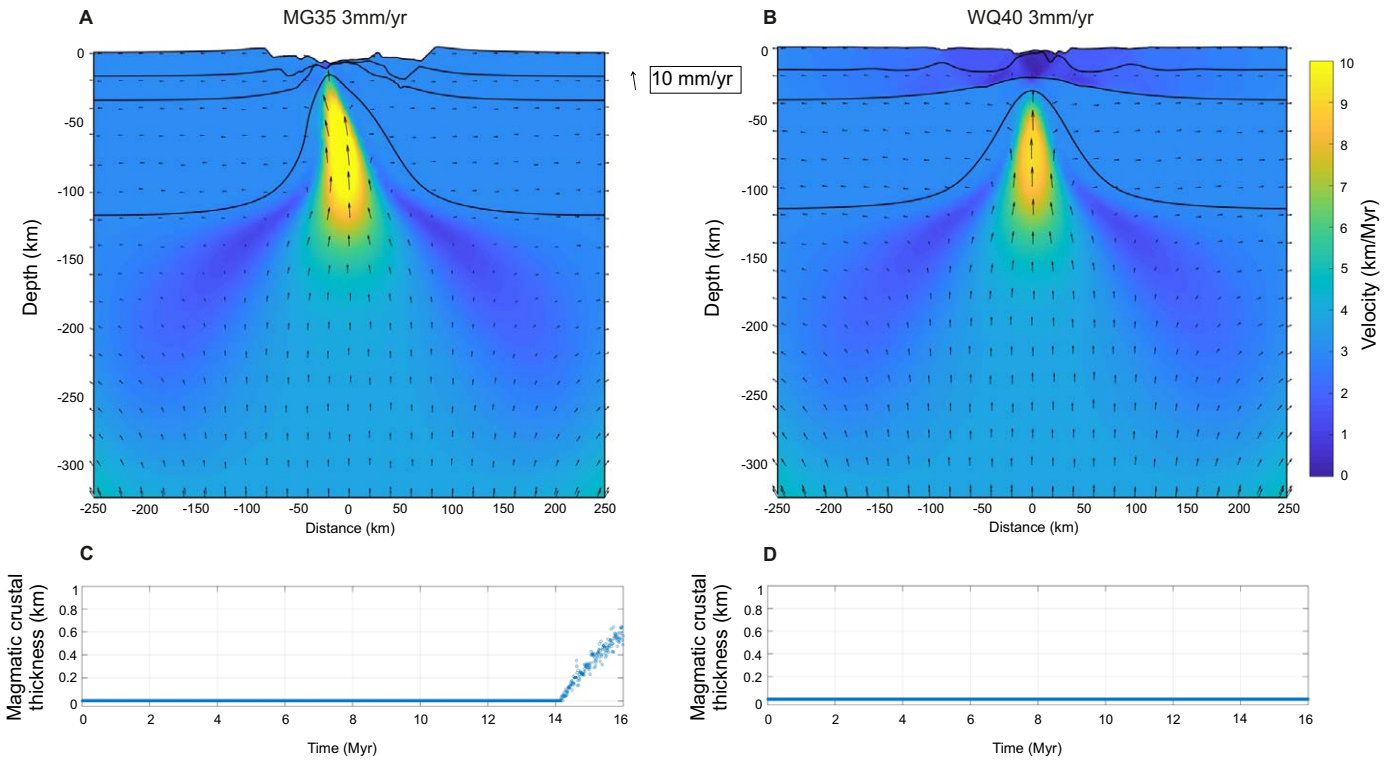

Figure 5. Velocity flow snapshot at 16 Myr after the onset of extension for the 3 mm/yr half-extension models: (a) MG35, mafic granulite lower crust and 35 km crustal thickness and (b) WQ40, wet quartzite lower crust and 40 km crustal thickness. Predicted magmatic crustal thickness from the onset of extension to 16 Myr after, for the 3 mm/yr half-extension models: (c) MG35 and (d) WQ40.

extended with the same velocity, the weak lower crust leads to a larger crust-mantle decoupling and slower uplift of the mantle than the strong lower crust model, which delays the onset of melting (Figure 5).

The dependence of predicted magmatic crustal thickness on crustal rheology over time is shown in Figure 4b. We have calculated the magmatic crustal thickness by assuming that all magma produced at each time step is accommodated in a dike beneath the Moho (see supporting information). For each velocity group, the onset of melting occurs earlier for strong lower crustal rheologies (mafic granulite) and it is delayed for larger decoupling between crust and mantle, which occurs with increasing crustal thickness or decreasing crustal strength (wet quartzite). For 3 mm/yr, the magmatic crustal thickness varies between 1 and 2 km depending on the crustal strength, whereas higher velocities of 5 and 10 mm/yr lead to magmatic thicknesses of 3.5 and 4.5 km respectively, regardless of the crustal rheology.

5.2. Linking Margin Tectonic Style and COT Nature

Our results suggest that margins where ductile processes dominate deformation are likely to be characterized by magma-dominated COTs with little to no serpentinized mantle, regardless of the extension velocity. This type of margin can be recognized by their large width, gentle continental slope and crustal tapering, small offset faults that dip both land- and oceanward and are indicative for the long periods on wide rifting mode, and little syn-rift subsidence (Figure 6). The delay between the onset of melting and that of serpentinization tends to be larger for wider margins (Figure 4a), indicating that the likelihood to find any serpentinized mantle in between magmatic products decreases as the margin width increases. The degree of symmetry is not symptomatic of the type of COT. However, asymmetric margins will be characterized by a thin layer of melt underplated mostly underneath the wide margin (Figure 6d), while at symmetric conjugate margins the level of magmatic underplating under both sides is similar (Figure 6c).

Margins characterized by strong crust, which leads to more brittle dominated deformation processes, show the onset of serpentinization prior to melting for very slow velocities ($<$ 5 mm/yr half-extension; Figure 4a). These margins are likely to be associated with a COT consisting of exhumed and serpentinized mantle

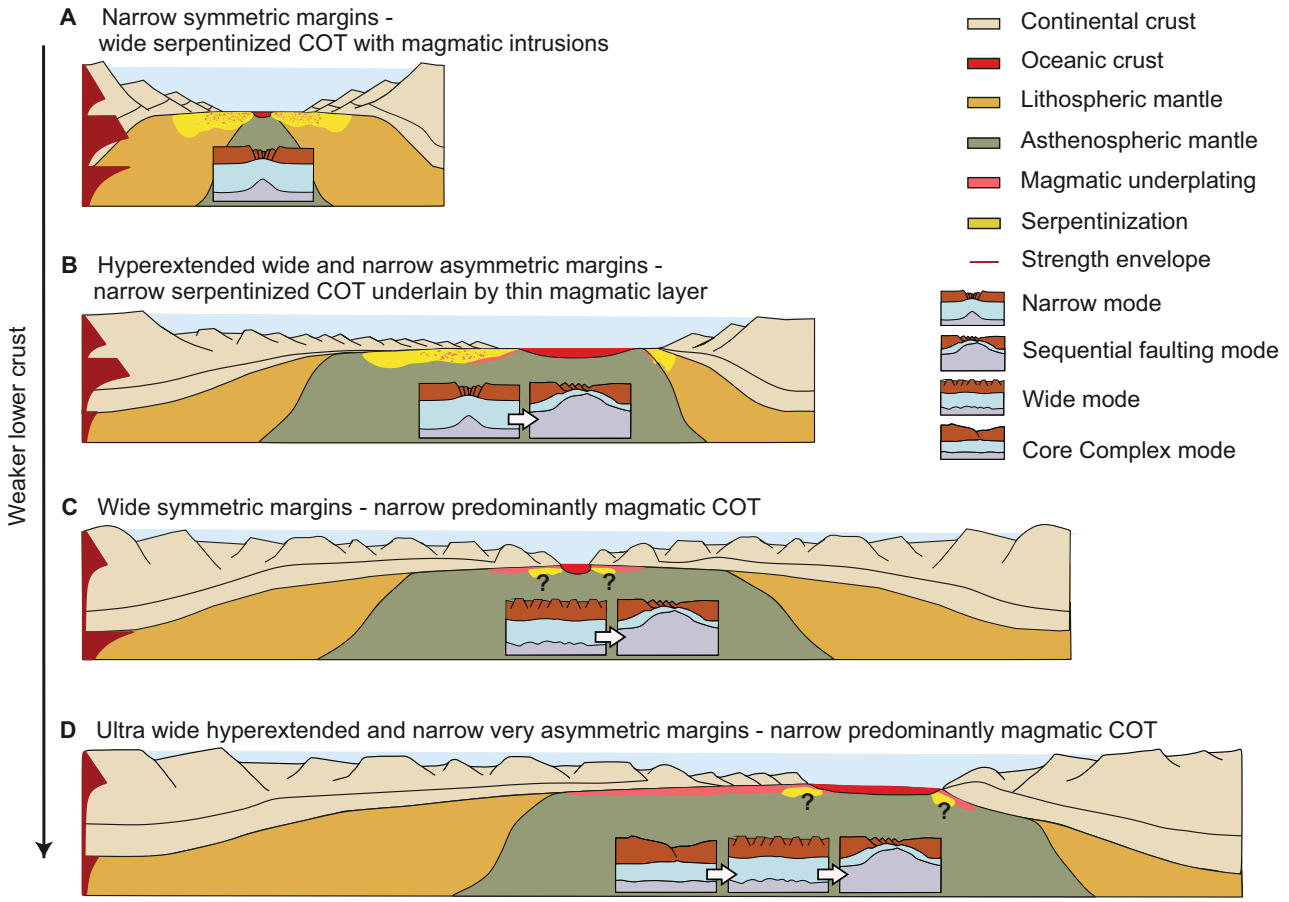

Figure 6. Conceptual model showing the genetic link between tectonic style and COT nature at magma-poor conjugate margins. Cartoons show break-up stage of the models extended by 3 mm/yr. Lower crustal strength ranges from strong (top plot a) to very weak (bottom panel D); (a)Mafic granulite and thin lower crust. (b) Mafic granulite and thick lower crust. (c) Wet quartzite and thin lower crust. (d) Wet quartzite and thick lower crust. Boxes show the mode evolution for each of the tectonic styles.

underplated by a thin layer of melt (Figures 6a and 6b). These margins can be recognized by large fault offsets ($>$ 5 km) defining the shelf break, abrupt crustal thinning, mainly oceanward dipping faults and large syn-rift subsidence. Symmetric margins tend to be narrow because large brittle faults are very effective at thinning the crust and causing quick break-up. Asymmetric margins are formed by tapping into deep levels of weak lower crust which prevents such rapid break-up by faulting and so become typically wider than symmetric ones. The onset of serpentinization occurs later for asymmetric than symmetric margins. Additionally, serpentinization under the thinned crust in asymmetric margins is mainly localized underneath the thinned crust of the wide margin, while it is more uniformly distributed underneath symmetric margins. The time gap between onset of serpentinization and that of melting is smaller for asymmetric margins (Figure 4a). Thus, the exhumed mantle at the COT probably presents more evidence of magmatism and may be narrower for asymmetric than for symmetric margins (Figures 6a and 6b).

In summary, we suggest that in order to understand margin evolution it will be useful to distinguish between margin sections that have gone through extensional modes of core-complex, wide, and narrow modes, since these have characteristic heat-flow and subsidence histories. This, in combination with rift migration accomplished by sequential faulting can explain the degree of asymmetry observed in conjugate margins (Figure 6). Our results support the idea that the development of a hyperextended crust is not necessarily related to the exhumation of lithospheric mantle, as described by Lau et al. (2015) for the East Orphan Basin, Cowie et al. (2017) for the Angolan margin and Evain et al. (2015) for the Santos Basin. Margins that undergo a prolonged phase of wide rifting tend to show a magmatic dominated COT, while those that undergo a dominant narrow extension phase, whether or not in combination with sequential faulting,

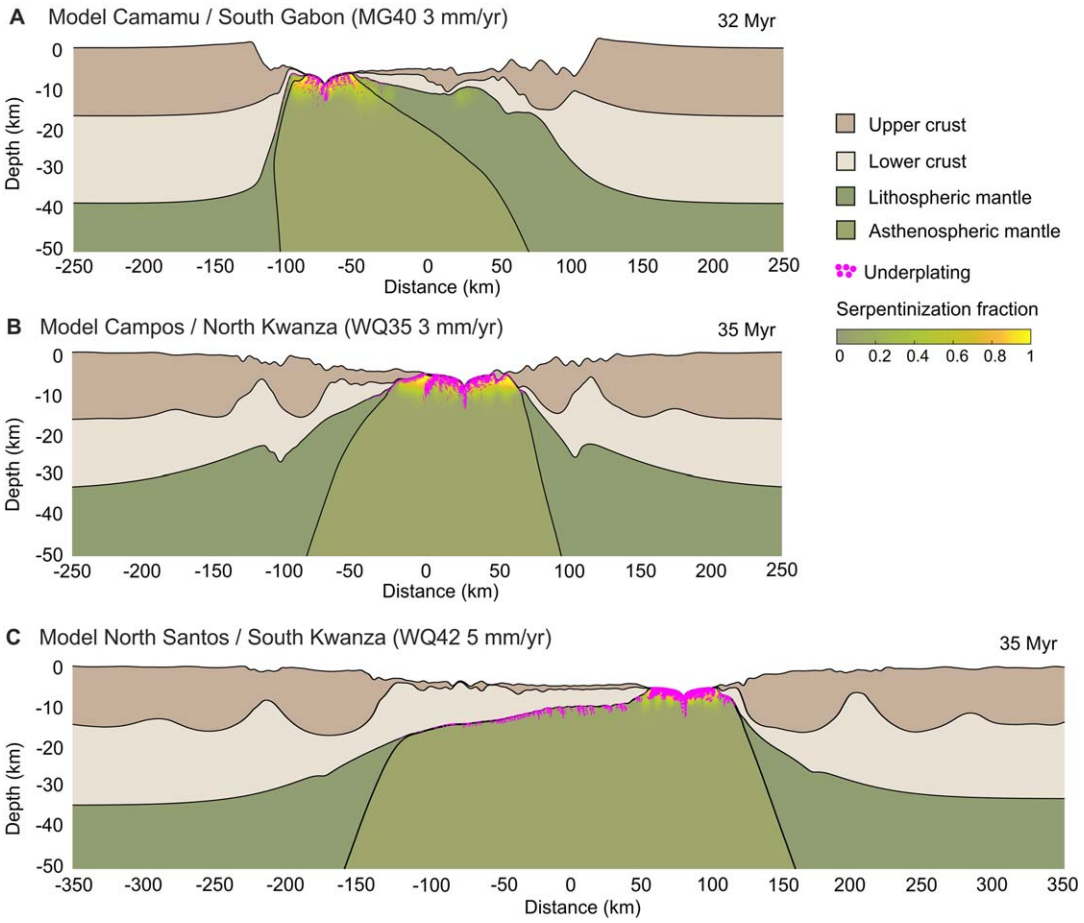

Figure 7. Compilation of the best-fit numerical models reproducing the main characteristics for the three seismic lines of the central South Atlantic segment. (a) Camamu/Gabon model (MG40: Mafic granulite, 40 km crustal thickness and 3 mm/yr extension). (b) Campos/North Kwanza model (WQ35: Wet quartzite, 35 km crustal thickness and 3 mm/yr extension). (c) North Santos/South Kwanza model (WQ42: Wet quartzite, 42 km crustal thickness and 5 mm/yr extension).

and those which extended very slowly ($<$ 5 mm/yr) tend to exhibit a COT consisting of exhumed serpentinized mantle (Figure 6).

5.3. Implications for the Central South Atlantic COTs

As we move southward along our study area, the conjugate margin-pair widths increase, while the continental slope and crustal tapering become gentler, indicating an increasing importance of ductile crustal deformation processes (Figure 2a). This suggests that the original lithosphere in which these margins developed was weaker to the South. The reason for a progressive weakening may either be a change in the lithology and amount of fluids of the lower crust, a thermal weakening in the South associated with the "Tristan da Cunha" plume that is linked to Paraná flood basalts, or a change in the lithospheric strength from the São Francisco craton in the North to the warmer and thinner Ribeira/Kaoko fold belts to the South. In this study we have chosen to reproduce the change in strength by changing only the crustal composition and thickness, as this gives us a good indication of margin tectonic style and COT nature with varying strength.

We have chosen three modeled sections to correlate the main characteristics of the transects shown in our study area (Figures 2 and 7). The Camamu/Gabon interpreted line shows an asymmetric structure with large, oceanward-dipping faults, abrupt crustal tapering, and large syn-rift subsidence, indicative for rifting in a strong crust (Figure 2a). We compare this line to the model with mafic granulite and 40 km crustal thickness extended by 3 mm/yr half-extension velocity (Heine et al., 2013). The initial conditions result in asymmetric conjugate margins with lateral dimensions and patterns of crustal thinning similar to those of the

observed section (Figures 2a and 7a). We suggest that the thinnest crust (< 3–4 km thick) along this conjugate margin transect may be underlain by serpentinized mantle with little magmatism. Serpentinized mantle is more likely to be found underneath the hyper-extended crust of the wide margin (the Gabon side) and the COT may present a narrow zone of exhumed serpentinized mantle (in comparison to the ~200 km of West Iberia, Minshull et al., 2014), with underplated magmatic products. This interpretation agrees with that of Clerc et al. (2017) for the Gabon COT, where their study suggests that it may consist of either be exhumed mantle or proto-oceanic crust, and that of Caixeta et al. (2009) for the Camamu basin who propose the occurrence of mantle exhumation at the COT, based on seismic, gravimetric and magnetometric data.

The model with weak wet quartzite lower crust, 35 km of crustal thickness and half-extension velocity of 3 mm/yr, is compared to the observations of the Campos/North Kwanza conjugate margins (Figures 2b and 7b). The geoseismic transect shows fairly symmetric conjugate margins, a moderate crustal tapering, small fault offsets dipping both land- and oceanward and little syn-rift subsidence, characteristics that are well reproduced by our model. The distal margins in our model show a break-up of the lithosphere mantle prior to upper-crustal break-up, as the Type II models of Huismans and Beaumont (2011, 2014), and the resulting COT is dominated by magma with an abrupt transition to oceanic crust. This interpretation for the COT is similar to the interpretation of the northern Angolan margin from Cowie et al. (2017), who suggested that it is a mix of hyperextended crust and magmatic material in basis of gravity modeling.

Along the North Santos/South Kwanza section the extension velocity is higher than to the North with approximately 5 mm/yr half-extension (Heine et al., 2013). We compare the section in this area (Figure 2c) to a model with wet quartzite lower crust, 42 km crustal thickness and 5 mm/yr (Figure 7c). This model results in a tectonic style quite similar to the case with 40 km crust, wet quartzite lower crust and 3 mm/yr (Figures 3j–3l and supporting information Movie S4). We chose to increase by 2km the input parameter of crustal thickness because the margins that resulted with 40 km were much narrower than those with 3 mm/yr, as the higher velocity led to a quicker localization and break-up. The 42 km crustal thickness is in the range of the onshore estimates for this area (Assumpção et al., 2013). The model results in a hyperextended margin that is 433 km wide and a 272 km wide conjugate, both margins thin from 42 to ~4.5 km. The wide hyperextended margin is slightly narrower than the observed in Santos; we follow other authors and suggest that the very large width of these margins results from a failed spreading center localized between the northern Pelotas Basin and the southern Santos Basin that cannot be reproduced in our 2-D models (Gomes et al., 2002; Mohriak, 2001; Moulin et al., 2013). Our model shows a very weak margin that goes through the extensional modes of core-complex, wide margin and finally rift migration accomplished by sequential faulting, as the lithospheric layers progressively cool and couple. Rifting lasts for a very long period of about 35 Myr, and it is characterized by very little syn-rift subsidence, perhaps providing the necessary conditions for the formation of a large salt basin. Faults are small, mostly dipping ocean- and landward, excluding those areas affected by the sequential faulting phase at the end of rifting. The Santos Basin in our model is underplated along most of its length by melt, while underplating is much less ubiquitous in the conjugate margin (Figure 7c). The COT is predominantly magmatic and the transition to standard oceanic crust is fairly abrupt. Although our result for the COT contrasts with the interpretation from Zalán et al. (2011), who suggested the exhumation of mantle based on the interpretation of multi-channel seismic lines, it coincides with the interpretations from Kumar et al. (2013), Aslanian et al. (2009) and Mohriak et al. (2008), who used the same type of data, and from Evain et al. (2015), who used multichannel and additional wide-angle seismic data to differentiate between various types of COT.

6. Conclusions

The above numerical models have shown different implications for the linkage between tectonic style and COT type of magma-poor conjugate rifted margins. During continental extension, a feedback between the rheology of the lower crust and the extension velocity strongly controls the onset of melting and serpentinization. The more decoupled the crust-mantle system, the greater the delay between the onsets of melting and serpentinization. This delay decreases with increasing extension velocity. Models with slow extension velocity (3 mm/yr) and strong mafic granulite lower crust show serpentinization prior to melting. We suggest that these models will present a COT characterized by exhumed and serpentinized mantle. In contrast, models

with weaker wet quartzite lower crust undergo an earlier onset of melting than serpentinization at all velocities tested here (3, 5 and 10 mm/yr half-extension), suggesting that a magmatically dominated COT would result.

The tectonic style of conjugate rifted margins (pattern of symmetry/asymmetry, margin width, pattern of faulting and subsidence) is strongly influenced by the strength of the lower crust, which confirms the results of previous studies (e.g., Brune et al., 2017; Tetreault & Buiter, 2017). Margin tectonic style can be explained by a combination of core-complex, wide and narrow rifting mode, as suggested by Buck (1991), combined with a fourth extensional mode, rift migration accomplished by sequential faulting (Brune et al., 2014, 2017; Ranero & Pérez-Gussinyé, 2010), which accounts for the observed degree of asymmetry.

The COT nature is linked to the tectonic style through the modes of extension that continental lithosphere undergoes, which in turn depend on the strength of lower crust and extension velocity. Strong lower crust leads to a development of large faults (offsets $> \sim$5 km) mainly dipping oceanward, abrupt crustal thinning, large syn-rift subsidence and the onset of serpentinization prior to melting, which results in a COT consisting of exhumed and serpentinized mantle. Weaker rheologies decrease the degree of coupling between crust and mantle promoting the generation of small faults (offsets $<$ 5 km) that dip both ocean- and landward, and that induce smooth crustal thinning and minor syn-rift subsidence. This type of deformation delays the onset of serpentinization more than it slows mantle upwelling and melting, so that melting starts before serpentinization at any velocity within the ultra-slow range, and leading to a more magmatic COT.

Our results predict a COT dominated by exhumed serpentinized mantle for strong lower crustal rheologies and slow velocities in the central South Atlantic segment (i.e., Camamu-Gabon conjugate margins) and a more magmatic COT with a rather abrupt transition to oceanic crust for weaker lower crustal rheologies and/or higher extension velocities (i.e., Campos-Kwanza and North Santos-South Kwanza conjugate margins). Therefore, our results show that magma-poor margins can exhibit COTs which lack exhumed and serpentinized mantle at their COT.

Acknowledgments
The authors thank COMPASS for the funding support. Elena Ros is grateful to Albert de Montserrat for his valuable discussions on the topic. We also thank S. Buiter, T. Minshull and L. Lavier for their valuable revisions which helped to improve the paper. The MCS data used in this study are proprietary data from ION-GXT. The data have been published before in several publications indicated in the text.

References

Andrés-Martínez, M., Morgan, J. P., Pérez-Gussinyé, M., & Rüpke, L. (2015). A new free-surface stabilization algorithm for geodynamical modelling: Theory and numerical tests. *Physics of the Earth and Planetary Interiors*, *246*, 41–51.

Araújo, M. N. C., Pérez-Gussinyé, M., & Romeiro, M. A. T. (2015). *A influência da taxa de deformaçao e reologia no estilo estrutural do rifte sul-Atlântico*. Paper presented at 9th International Symposium on Tectonics, Brazilian Geological Society, Salvador, Brazil.

Armitage, J. J., Henstock, T. J., Minshull, T. A., & Hopper, J. R. (2009). Lithospheric controls on melt production during continental breakup at slow rates of extension: Application to the North Atlantic. *Geochemistry, Geophysics, Geosystems*, *10*, Q06018. https://doi.org/10.1029/2009GC002404

Armitage, J. J., Jaupart, C., Fourel, L., & Allen, P. A. (2013). The instability of continental passive margins and its effect on continental topography and heat flow. *Journal of Geophysical Research: Solid Earth*, *118*, 1817–1836. https://doi.org/10.1002/jgrb.50097

Aslanian, D., Moulin, M., Olivet, J. L., Unternehr, P., Matias, L., Bache, F., . . . Labails, C. (2009). Brazilian and African passive margins of the Central Segment of the South Atlantic Ocean: Kinematic constraints. *Tectonophysics*, *468*(1), 98–112.

Assumpção, M., Bianchi, M., Julià, J., Dias, F. L., França, G. S., Nascimento, R., . . . Lopes, A. E. (2013). Crustal thickness map of Brazil: Data compilation and main features. *Journal of South American Earth Sciences*, *43*, 74–85.

Autin, J., Leroy, S., Beslier, M. O., D'acremont, E., Razin, P., Ribodetti, A., . . . Al Toubi, K. (2010). Continental break-up history of a deep magma-poor margin based on seismic reflection data (northeastern Gulf of Aden margin, offshore Oman). *Geophysical Journal International*, *180*(2), 501–519.

Bassi, G. (1991). Factors controlling the style of continental rifting: Insights from numerical modelling. *Earth and Planetary Science Letters*, *105*(4), 430–452.

Bassi, G. (1995). Relative importance of strain rate and rheology for the mode of continental extension. *Geophysical Journal International*, *122*(1), 195–210.

Bassi, G., Keen, C. E., & Potter, P. (1993). Contrasting styles of rifting: Models and examples from the eastern Canadian margin. *Tectonics*, *12*(3), 639–655.

Bayrakci, G., Minshull, T. A., Sawyer, D. S., Reston, T. J., Klaeschen, D., Papenberg, C., & Perez-Gussinye, M. (2016). Fault-controlled hydration of the upper mantle during continental rifting. *Nature Geoscience*, *9*(5), 384–388.

Beard, J. S., & Hopkinson, L. (2000). A fossil, serpentinization-related hydrothermal vent, Ocean Drilling Program Leg 173, Site 1068 (Iberia Abyssal Plain): Some aspects of mineral and fluid chemistry. *Journal of Geophysical Research*, *105*(B7), 16527–16539.

Beaumont, C., & Ings, S. J. (2012). Effect of depleted continental lithosphere counterflow and inherited crustal weakness on rifting of the continental lithosphere: General results. *Journal of Geophysical Research*, *117*, B08407. https://doi.org/10.1029/2012JB009203

Bird, D. E., & Hall, S. A. (2016). Early seafloor spreading in the South Atlantic: New evidence for M-series magnetochrons north of the Rio Grande Fracture Zone. *Geophysical Journal International*, *206*(2), 835–844.

Blaich, O. A., Faleide, J. I., & Tsikalas, F. (2011). Crustal breakup and continent-ocean transition at South Atlantic conjugate margins. *Journal of Geophysical Research*, *116*, B01402. https://doi.org/10.1029/2010JB007686

Blaich, O. A., Faleide, J. I., Tsikalas, F., Lilletveit, R., Chiossi, D., Brockbank, P., & Cobbold, P. (2010). January). Structural architecture and nature of the continent-ocean transitional domain at the Camamu and Almada Basins (NE Brazil) within a conjugate margin setting. In *Geological Society, London, Petroleum geology conference series* (Vol. 7, No. 1, pp. 867–883). London, UK: Geological Society of London.

Boillot, G., Winterer, E. L., Meyer, A. W., et al. (1987). In *Proceedings of the Ocean Drilling Program, initial reports* (Vol. 103). College Station, TX: Ocean Drilling Program. https://doi.org/10.2973/odp.proc.ir.103.1987

Bos, B., & Spiers, C. J. (2002). Frictional-viscous flow of phyllosilicate-bearing fault rock: Microphysical model and implications for crustal strength profiles. *Journal of Geophysical Research*, *107*(B2), 2028. https://doi.org/10.1029/2001JB000301
Bown, J. W., & White, R. S. (1995). Effect of finite extension rate on melt generation at rifted continental margins. *Journal of Geophysical Research*, *100*(B9), 18011–18029.
Brune, S., Heine, C., Clift, P. D., & Pérez-Gussinyé, M. (2017). Rifted margin architecture and crustal rheology: Reviewing Iberia-Newfoundland, Central South Atlantic, and South China Sea. *Marine and Petroleum Geology*, *79*, 257–281.
Brune, S., Heine, C., Pérez-Gussinyé, M., & Sobolev, S. V. (2014). Rift migration explains continental margin asymmetry and crustal hyper-extension. *Nature Communications*, *5*.
Buck, W. R. (1991). Modes of continental lithospheric extension. *Journal of Geophysical Research*, *96*(B12), 20161–20178.
Buck, W. R., & Lavier, L. L. (2001). A tale of two kinds of normal fault: The importance of strain weakening in fault development. *Geological Society, Special Publications*, *187*(1), 289–303.
Buck, W. R., & Poliakov, A. N. (1998). Abyssal hills formed by stretching oceanic lithosphere. *Nature*, *392*(6673), 272–275.
Buiter, S. J., Huismans, R. S., & Beaumont, C. (2008). Dissipation analysis as a guide to mode selection during crustal extension and implications for the styles of sedimentary basins. *Journal of Geophysical Research*, *113*, B06406. https://doi.org/10.1029/2007JB005272
Burov, E. B. (2011). Rheology and strength of the lithosphere. *Marine and Petroleum Geology*, *28*(8), 1402–1443.
Caixeta, J. M., Ferreira, T. S., Lima, F. D., Francisco, C., & Dias, A. (2009). APPG International Conference & Exhibition (15–18 November 2009, Rio de Janeiro, Brazil), Diachronous rift system along Bahia State coast: An example of extended crust and mantle exhumation in the South Atlantic Ocean. AAPG Search and Discovery Article #90100.
Cannat, M., Manatschal, G., Sauter, D., & Peron-Pinvidic, G. (2009). Assessing the conditions of continental breakup at magma-poor rifted margins: What can we learn from slow spreading mid-ocean ridges? *Comptes Rendus Geoscience*, *341*(5), 406–427.
Chian, D. P., Louden, K. E., Minshull, T. A., & Whitmarsh, R. B. (1999). Deep structure of the ocean-continent transition in the southern Iberia Abyssal Plain from seismic refraction profiles: Ocean Drilling Program (Legs 149 and 173) transect. *Journal of Geophysical Research*, 104(B4), 7443–7462.
Clerc, C., Ringenbach, J. C., Jolivet, L., & Ballard, J. F. (2017). Rifted margins: Ductile deformation, boudinage, continentward-dipping normal faults and the role of the weak lower crust. *Gondwana Research*. https://doi.org/10.1016/j.gr.2017.04.030, in press.
Cowie, L., Angelo, R. M., Kusznir, N., Manatschal, G., & Horn, B. (2017). Structure of the ocean–continent transition, location of the continent–ocean boundary and magmatic type of the northern Angolan margin from integrated quantitative analysis of deep seismic reflection and gravity anomaly data. *Geological Society, Special Publications*, *438*(1), 159–176.
Currie, C. A., & Hyndman, R. D. (2006). The thermal structure of subduction zone back arcs. *Journal of Geophysical Research*, *111*, B08404. https://doi.org/10.1029/2005JB004024
Dabrowski, M., Krotkiewski, M., & Schmid, D. W. (2008). MILAMIN: MATLAB-based finite element method solver for large problems. *Geochemistry, Geophysics, Geosystems*, *9*, Q04030. https://doi.org/10.1029/2007GC001719
De Bresser, J., Ter Heege, J., & Spiers, C. (2001). Grain size reduction by dynamic recrystallization: Can it result in major rheological weakening?. *International Journal of Earth Sciences*, *90*(1), 28–45.
Dick, H. J., Lin, J., & Schouten, H. (2003). An ultraslow-spreading class of ocean ridge. *Nature*, *426*(6965), 405–412.
Direen, N. G., Borissova, I., Stagg, H. M. J., Colwell, J. B., & Symonds, P. A. (2007). Nature of the continent–ocean transition zone along the southern Australian continental margin: A comparison of the Naturaliste Plateau, SW Australia, and the central Great Australian Bight sectors. *Geological Society, Special Publications*, *282*(1), 239–263.
Direen, N. G., Stagg, H. M., Symonds, P. A., & Norton, I. O. (2013). Variations in rift symmetry: Cautionary examples from the Southern Rift System (Australia–Antarctica). *Geological Society, Special Publications*, *369*(1), 453–475.
Dunbar, J. A., & Sawyer, D. S. (1989). How preexisting weaknesses control the style of continental breakup. *Journal of Geophysical Research*, *94*(B6), 7278–7292.
Eagles, G. (2007). New angles on South Atlantic opening. *Geophysical Journal International*, *168*(1), 353–361.
Eagles, G., Pérez-Díaz, L., & Scarselli, N. (2015). Getting over continent ocean boundaries. *Earth-Science Reviews*, *151*, 244–265.
Emmanuel, S., & Berkowitz, B. (2006). Suppression and stimulation of seafloor hydrothermal convection by exothermic mineral hydration. *Earth and Planetary Science Letters*, *243*(3), 657–668.
Escartin, J., Hirth, G., & Evans, B. (1997). Effects of serpentinization on the lithospheric strength and the style of normal faulting at slow-spreading ridges. *Earth and Planetary Science Letters*, *151*(3–4), 181–189.
Evain, M., Afilhado, A., Rigoti, C., Loureiro, A., Alves, D., Klingelhoefer, F., . . . Lima, M. V. (2015). Deep structure of the Santos Basin-São Paulo Plateau System, SE Brazil. *Journal of Geophysical Research: Solid Earth*, *120*, 5401–5431. https://doi.org/10.1002/2014JB011561
Feng, M., Van der Lee, S., & Assumpção, M. (2007). Upper mantle structure of South America from joint inversion of waveforms and fundamental mode group velocities of Rayleigh waves. *Journal of Geophysical Research*, *112*, B04312. https://doi.org/10.1029/2006JB004449
Ferreira, T. S., Caixeta, J. M., & Lima, F. D. (2009). Controle do embasamento no rifteamento das bacias de Camamu e Almada. *Boletim De Geociências Da Petrobras, Rio De Janeiro*, *17*(1), 69–88.
Gleason, G. C., & Tullis, J. (1995). A flow law for dislocation creep of quartz aggregates determined with the molten salt cell. *Tectonophysics*, *247*(1), 1–23.
Gomes, P. O., Parry, J., & Martins, W. (2002). September). The outer high of the Santos Basin, southern Sao Paulo Plateau, Brazil: Tectonic setting, relation to volcanic events and some comments on hydrocarbon potential. In *AAPG Hedberg Conference on hydrocarbon habitat of volcanic rifted passive margins* (pp. 8–11). American Association of Petroleum Gelogists.
Groupe Galice (1979). The continental margin off Galicia and Portugal: Acoustical stratigraphy, dredge stratigraphy, and structural evolution, *Initial Reports Deep Sea Drilling Project*, *47*(Part 2), 633–662.
Gudmundsson, A. (1990). Emplacement of dikes, sills and crustal magma chambers at divergent plate boundaries. *Tectonophysics*, *176*(3–4), 257–275.
Gudmundsson, A. (2011). Deflection of dykes into sills at discontinuities and magma-chamber formation. *Tectonophysics*, *500*(1), 50–64.
Heilbron, M., Valeriano, C. M., Tassinari, C. C. G., Almeida, J., Tupinambá, M., Siga, O., & Trouw, R. (2008). Correlation of Neoproterozoic terranes between the Ribeira Belt, SE Brazil and its African counterpart: Comparative tectonic evolution and open questions. *Geological Society, Special Publications*, *294*(1), 211–237.
Heine, C., Zoethout, J., & Müller, R. D. (2013). Kinematics of the South Atlantic rift. *Solid Earth*, *4*(2), 215–253.
Hirth, G., & Kohlstedt, D. (2003). Rheology of the upper mantle and the mantle wedge: A view from the experimentalists. In J. Eiler (Ed.), *Inside the Subduction Factory* (pp. 83–105). Washington, DC: American Geophysical Union.
Hirth, G., & Kohlstedt, D. L. (1996). Water in the oceanic upper mantle: Implications for rheology, melt extraction and the evolution of the lithosphere. *Earth and Planetary Science Letters*, *144*(1–2), 93–108.

Hopper, J. R., & Buck, W. R. (1996). and passive margin formation. *Journal of Geophysical Research*, *101*(B9), 20–175.
Huismans, R., & Beaumont, C. (2011). Depth-dependent extension, two-stage breakup and cratonic underplating at rifted margins. *Nature*, *473*(7345), 74–78.
Huismans, R. S., & Beaumont, C. (2002). Asymmetric lithospheric extension: The role of frictional plastic strain softening inferred from numerical experiments. *Geology*, *30*(3), 211–214.
Huismans, R. S., & Beaumont, C. (2014). Rifted continental margins: The case for depth-dependent extension. *Earth and Planetary Science Letters*, *407*, 148–162.
Ito, G., Lin, J., & Gable, C. W. (1996). Dynamics of mantle flow and melting at a ridge-centered hotspot: Iceland and the Mid-Atlantic Ridge. *Earth and Planetary Science Letters*, *144*(1–2), 53–74.
Iyer, K. (2007). *Mechanisms of serpentinization and some geochemical effects* (Doctoral dissertation). Oslo, Norway: University of Oslo.
Jokat, W., Ritzmann, O., Schmidt-Aursch, M. C., Drachev, S., Gauger, S., & Snow, J. (2003). Geophysical evidence for reduced melt production on the Arctic ultraslow Gakkel mid-ocean ridge. *Nature*, *423*(6943), 962–965.
Katayama, I., Hirauchi, K. I., Michibayashi, K., & Ando, J. I. (2009). Trench-parallel anisotropy produced by serpentine deformation in the hydrated mantle wedge. *Nature*, *461*(7267), 1114–1117.
Kaus, B. J., Mühlhaus, H., & May, D. A. (2010). A stabilization algorithm for geodynamic numerical simulations with a free surface. *Physics of the Earth and Planetary Interiors*, *181*(1), 12–20.
Kawano, S., Katayama, I., & Okazaki, K. (2011). Permeability anisotropy of serpentinite and fluid pathways in a subduction zone. *Geology*, *39*(10), 939–942.
Klein, F., Humphris, S. E., Guo, W., Schubotz, F., Schwarzenbach, E. M., & Orsi, W. D. (2015). Fluid mixing and the deep biosphere of a fossil Lost City-type hydrothermal system at the Iberia Margin. *Proceedings of the National Academy of Sciences United States of America*, *112*(39), 12036–12041.
Kumar, N., Danforth, A., Nuttall, P., Helwig, J., Bird, D. E., & Venkatraman, S. (2013). From oceanic crust to exhumed mantle: A 40 year (1970–2010) perspective on the nature of crust under the Santos Basin, SE Brazil. *Geological Society, Special Publications*, *369*(1), 147–165.
Lau, K. H., Watremez, L., Louden, K. E., & Nedimović, M. R. (2015). Structure of thinned continental crust across the Orphan Basin from a dense wide-angle seismic profile and gravity data. *Geophysical Journal International*, *202*(3), 1969–1992.
Lavecchia, A., Thieulot, C., Beekman, F., Cloetingh, S., & Clark, S. (2017). Lithosphere erosion and continental breakup: Interaction of extension, plume upwelling and melting. *Earth and Planetary Science Letters*, *467*, 89–98.
Lavier, L. L., Buck, W. R., & Poliakov, A. N. (1999). Self-consistent rolling-hinge model for the evolution of large-offset low-angle normal faults. *Geology*, *27*(12), 1127–1130.
Lavier, L. L., & Manatschal, G. (2006). A mechanism to thin the continental lithosphere at magma-poor margins. *Nature*, *440*(7082), 324–328.
Lemoine, M., Bas, T., Arnaud-Vanneau, A., Arnaud, H., Dumont, T., Gidon, M., . . . Tricart, P. (1986). The continental margin of the Mesozoic Tethys in the Western Alps. *Marine and Petroleum Geology*, *3*(3), 179–199.
Lentini, M. R., Fraser, S. I., Sumner, H. S., & Davies, R. J. (2010). Geodynamics of the central South Atlantic conjugate margins: Implications for hydrocarbon potential. *Petroleum Geoscience*, *16*(3), 217–229.
Lu, G., Kaus, B. J., & Zhao, L. (2011). Thermal localization as a potential mechanism to rift cratons. *Physics of the Earth and Planetary Interiors*, *186*(3), 125–137.
Macdonald, A. H., & Fyfe, W. S. (1985). Rate of serpentinization in seafloor environments. *Tectonophysics*, *116*(1–2), 123–135.
Malvern, L. E. (1969). *Introduction to the mechanics of a continuous medium* (monograph).
Manatschal, G. (2004). New models for evolution of magma-poor rifted margins based on a review of data and concepts from West Iberia and the Alps. *International Journal of Earth Sciences*, *93*(3), 432–466.
Manatschal, G., & Müntener, O. (2009). A type sequence across an ancient magma-poor ocean-continent transition: The example of the western Alpine Tethys ophiolites. *Tectonophysics*, *473*, 4–19.
Masini, E., Manatschal, G., & Mohn, G. (2012b). The Alpine Tethys rifted margins: Reconciling old and new ideas to understand the stratigraphic architecture of magma-poor rifted margins. *Sedimentology*, *60*(1), 174–196.
Mathieu, L., De Vries, B. V. W., Holohan, E. P., & Troll, V. R. (2008). Dykes, cups, saucers and sills: Analogue experiments on magma intrusion into brittle rocks. *Earth and Planetary Science Letters*, *271*(1), 1–13.
Minshull, T. A. (2009). Geophysical characterisation of the ocean–continent transition at magma-poor rifted margins. *Comptes Rendus Geoscience*, *341*(5), 382–393.
Minshull, T. A., Dean, S. M., White, R. S., & Whitmarsh, R. B. (2001). Anomalous melt production after continental break-up in the southern Iberia Abyssal Plain. *Geological Society, Special Publications*, *187*(1), 537–550.
Minshull, T. A., Dean, S. M., & Whitmarsh, R. B. (2014). The peridotite ridge province in the southern Iberia Abyssal Plain: Seismic constraints revisited. *Journal of Geophysical Research: Solid Earth*, *119*, 1580–1598. https://doi.org/10.1002/2014JB011011
Mohn, G., Manatschal, G., Beltrando, M., Masini, E., & Kusznir, N. (2012). Necking of continental crust in magma-poor rifted margins: Evidence from the fossil Alpine Tethys margins. *Tectonics*, *31*, TC1012. https://doi.org/10.1029/2011TC002961
Mohn, G., Manatschal, G., Müntener, O., Beltrando, M., & Masini, E. (2010). Unravelling the interaction between tectonic and sedimentary processes during lithospheric thinning in the Alpine Tethys margins. *International Journal of Earth Sciences*, *99*(1), 75–101.
Mohriak, W., Nemčok, M., & Enciso, G. (2008). South Atlantic divergent margin evolution: Rift-border uplift and salt tectonics in the basins of SE Brazil. *Geological Society, Special Publications*, *294*(1), 365–398.
Mohriak, W. U. (2001, October). South Atlantic ocean salt tectonics, volcanic centers, fracture zones and their relationship with the origin and evolution of the South Atlantic Ocean: Geophysical evidence in the Brazilian and West African Margins. In *7th International Congress of the Brazilian Geophysical Society*.
Mohriak, W. U., Szatmari, P., & Anjos, S. (2012). Salt: Geology and tectonics of selected Brazilian basins in their global context. *Geological Society, Special Publications*, *363*(1), 131–158.
Morgan, J. P. (1987). Melt migration beneath mid-ocean spreading centers. *Geophysical Research Letters*, *14*(12), 1238–1241.
Morgan, J. P. (1997). The generation of a compositional lithosphere by mid-ocean ridge melting and its effect on subsequent off-axis hotspot upwelling and melting. *Earth and Planetary Science Letters*, *146*(1–2), 213–232.
Morgan, J. P. (2001). Thermodynamics of pressure release melting of a veined plum pudding mantle. *Geochemistry, Geophysics, Geosystems*, *2*(4), 1001. https://doi.org/10.1029/2000GC000049
Moulin, M., Aslanian, D., Rabineau, M., Patriat, M., & Matias, L. (2013). Kinematic keys of the Santos–Namibe basins. *Geological Society, Special Publications*, *369*(1), 91–107.
Müntener, O., Hermann, J., & Trommsdorff, V. (2000). Cooling history and exhumation of lower-crustal granulite and upper mantle (Malenco, Eastern Central Alps). *Journal of Petrology*, *41*(2), 175–200.

Nagel, T. J., & Buck, W. R. (2004). Symmetric alternative to asymmetric rifting models. *Geology*, *32*(11), 937–940.
Naliboff, J., & Buiter, S. J. (2015). Rift reactivation and migration during multiphase extension. *Earth and Planetary Science Letters*, *421*, 58–67.
ODP Leg 173 Shipboard Scientific Party (1998). Drilling reveals transition from continental breakup to early magmatic crust. *Eos, Transactions American Geophysical Union*, *79*(173), 180–181.
Osmundsen, P. T., & Ebbing, J. (2008). Styles of extension offshore mid-Norway and implications for mechanisms of crustal thinning at passive margins. *Tectonics*, *27*, TC6016. https://doi.org/10.1029/2007TC002242
Pérez-Díaz, L., & Eagles, G. (2014). Constraining South Atlantic growth with seafloor spreading data. *Tectonics*, *33*, 1848–1873. https://doi.org/10.1002/2014TC003644
Pérez-Gussinyé, M., Lowry, A. R., & Watts, A. B. (2007). Effective elastic thickness of South America and its implications for intracontinental deformation. *Geochemistry, Geophysics, Geosystems*, *8*, Q05009. https://doi.org/10.1029/2006GC001511
Pérez-Gussinyé, M., Metois, M., Fernández, M., Vergés, J., Fullea, J., & Lowry, A. R. (2009). Effective elastic thickness of Africa and its relationship to other proxies for lithospheric structure and surface tectonics. *Earth and Planetary Science Letters*, *287*(1), 152–167.
Pérez-Gussinyé, M., Morgan, J. P., Reston, T. J., & Ranero, C. R. (2006). The rift to drift transition at non-volcanic margins: Insights from numerical modelling. *Earth and Planetary Science Letters*, *244*(1), 458–473.
Pérez-Gussinyé, M., & Reston, T. J. (2001). Rheological evolution during extension at nonvolcanic rifted margins: Onset of serpentinization and development of detachments leading to continental breakup. *Journal of Geophysical Research*, *106*(B3), 3961–3975.
Peron-Pinvidic, G., Manatschal, G., Masini, E., Sutra, E., Flament, J. M., Haupert, I., & Unternehr, P. (2017). Unravelling the along-strike variability of the Angola–Gabon rifted margin: A mapping approach. *Geological Society, Special Publications*, *438*(1), 49–76.
Péron-Pinvidic, G., Manatschal, G., Minshull, T. A., & Sawyer, D. S. (2007). Tectonosedimentary evolution of the deep Iberia-Newfoundland margins: Evidence for a complex breakup history. *Tectonics*, *26*, TC2011. https://doi.org/10.1029/2006TC001970
Pinto, V. H. G., Manatschal, G., Karpoff, A. M., Ulrich, M., & Viana, A. R. (2017). Seawater storage and element transfer associated with mantle serpentinization in magma-poor rifted margins: A quantitative approach. *Earth and Planetary Science Letters*, *459*, 227–237.
Pinto, V. H. G., Manatschal, G., Karpoff, A. M., & Viana, A. (2015). Tracing mantle-reacted fluids in magma-poor rifted margins: The example of Alpine Tethyan rifted margins. *Geochemistry, Geophysics, Geosystems*, *16*, 3271–3308. https://doi.org/10.1002/2015GC005830
Précigout, J., & Gueydan, F. (2009). Mantle weakening and strain localization: Implications for the long-term strength of the continental lithosphere. *Geology*, *37*(2), 147–150.
Ranalli, G. (1995). *Rheology of the earth*. the Netherlands: Springer Science and Business Media.
Ranalli, G., & Murphy, D. C. (1987). Rheological stratification of the lithosphere. *Tectonophysics*, *132*(4), 281–295.
Ranero, C. R., & Pérez-Gussinyé, M. (2010). Sequential faulting explains the asymmetry and extension discrepancy of conjugate margins. *Nature*, *468*(7321), 294–299.
Reston, T. J. (2009). The structure, evolution and symmetry of the magma-poor rifted margins of the North and Central Atlantic: A synthesis. *Tectonophysics*, *468*(1), 6–27.
Reston, T. J., Krawczyk, C. M., & Klaeschen, D. (1996). The S reflector west of Galicia (Spain): Evidence from prestack depth migration for detachment faulting during continental breakup. *Journal of Geophysical Research*, *101*(B4), 8075–8091.
Rüpke, L., Phipps Morgan, J., & Eaby Dixon, J. (2006). Implications of subduction rehydration for earth's deep water cycle. In S. D. Jacobsen & S. Van Der Lee (Eds.), *Earth's deep water cycle* (pp. 263–276). Washington, DC: American Geophysical Union.
Russell, S. M., & Whitmarsh, R. B. (2003). Magmatism at the west Iberia non-volcanic rifted continental margin: Evidence from analyses of magnetic anomalies. *Geophysical Journal International*, *154*(3), 706–730.
Sawyer, D. S., Whitmarsh, R. B., Klaus, A., et al. (1994). In *Proceedings of Ocean Drilling Program, initial reports* (Vol. 149). College Station, TX: Ocean Drilling Program. https://doi.org/10.2973/odp.proc.ir.149.1994
Sawyer, D. S., Coffin, M. F., Reston, T. J., Stock, J. M., & Hopper, J. R. (2007). COBBOOM: The continental breakup and birth of oceans mission. *Scientific Drilling*, *5*, 13–25.
Schmeling, H. (2010). Dynamic models of continental rifting with melt generation. *Tectonophysics*, *480*(1), 33–47.
Schrenk, M. O., Brazelton, W. J., & Lang, S. Q. (2013). Serpentinization, carbon, and deep life. *Reviews in Mineralogy and Geochemistry*, *75*(1), 575–606.
Sharples, W., Moresi, L. N., Jadamec, M. A., & Revote, J. (2015). Styles of rifting and fault spacing in numerical models of crustal extension. *Journal of Geophysical Research: Solid Earth*, *120*, 4379–4404. https://doi.org/10.1002/2014JB011813
Sibuet, J. C., Srivastava, S., & Manatschal, G. (2007). Exhumed mantle-forming transitional crust in the Newfoundland-Iberia rift and associated magnetic anomalies. *Journal of Geophysical Research*, *112*, B06105. https://doi.org/10.1029/2005JB003856
Sibuet, J. C., & Tucholke, B. E. (2013). The geodynamic province of transitional lithosphere adjacent to magma-poor continental margins. *Geological Society, Special Publications*, *369*(1), 429–452.
Simon, K., Huismans, R. S., & Beaumont, C. (2009). Dynamical modelling of lithospheric extension and small-scale convection: Implications for magmatism during the formation of volcanic rifted margins. *Geophysical Journal International*, *176*(1), 327–350.
Skelton, A., Whitmarsh, R., Arghe, F., Crill, P., & Koyi, H. (2005). Constraining the rate and extent of mantle serpentinization from seismic and petrological data: Implications for chemosynthesis and tectonic processes. *Geofluids*, *5*(3), 153–164.
Sotin, C., & Parmentier, E. M. (1989). Dynamical consequences of compositional and thermal density stratification beneath spreading centers. *Geophysical Research Letters*, *16*(8), 835–838.
Svartman Dias, A. E., Lavier, L. L., & Hayman, N. W. (2015). Conjugate rifted margins width and asymmetry: The interplay between lithospheric strength and thermomechanical processes. *Journal of Geophysical Research: Solid Earth*, *120*, 8672–8700. https://doi.org/10.1002/2015JB012074
Taylor, B., Goodliffe, A. M., & Martinez, F. (1999). How continents break up: Insights from Papua New Guinea. *Journal of Geophysical Research*, *104*(B4), 7497–7512.
Tetreault, J. L., & Buiter, S. J. H. (2017). The influence of extension rate and crustal rheology on the evolution of passive margins from rifting to break-up. *Tectonophysics*.
Thybo, H., & Artemieva, I. M. (2013). Moho and magmatic underplating in continental lithosphere. *Tectonophysics*, *609*, 605–619.
Tirel, C., Brun, J. P., & Burov, E. (2008). Dynamics and structural development of metamorphic core complexes. *Journal of Geophysical Research*, *113*, B04403. https://doi.org/10.1029/2005JB003694
Tucholke, B. E., Sawyer, D. S., & Sibuet, J. C. (2007). Breakup of the Newfoundland–Iberia rift. *Geological Society, Special Publications*, *282*(1), 9–46.
Tucholke, B. E., & Sibuet, J. C. (2007). Leg 210 synthesis: Tectonic, magmatic, and sedimentary evolution of the Newfoundland-Iberia rift. In *Proceedings of the Ocean Drilling Program, scientific results* (Vol. 210, pp. 1–56). College Station, TX: Ocean Drilling Program.
Unternehr, P., Péron-Pinvidic, G., Manatschal, G., & Sutra, E. (2010). Hyper-extended crust in the South Atlantic: In search of a model. *Petroleum Geoscience*, *16*(3), 207–215.

Welford, J. K., Hall, J., Sibuet, J. C., & Srivastava, S. P. (2010). Structure across the northeastern margin of Flemish Cap, offshore Newfoundland from Erable multichannel seismic reflection profiles: Evidence for a transtensional rifting environment. *Geophysical Journal International*, *183*(2), 572–586.

White, R. S., Minshull, T. A., Bickle, M. J., & Robinson, C. J. (2001). Melt generation at very slow-spreading oceanic ridges: Constraints from geochemical and geophysical data. *Journal of Petrology*, *42*(6), 1171–1196.

Whitmarsh, R. B., Beslier, M.-O., Wallace, P. J., et al. (1998). In *Proceedings of Ocean Drilling Program, initial reports* (Vol. 173). College Station, TX: Ocean Drilling Program. https://doi.org/10.2973/odp.proc.ir.173.1998

Whitmarsh, R. B., & Miles, P. R. (1995). Models of the development of the West Iberia rifted continental margin at 40° 30′ N deduced from surface and deep-tow magnetic anomalies. *Journal of Geophysical Research*, *100*(B3), 3789–3806.

Whitmarsh, R. B., White, R. S., Horsefield, S. J., Sibuet, J. C., Recq, M., & Louvel, V. (1996). The ocean-continent boundary off the western continental margin of Iberia: Crustal structure west of Galicia Bank. *Journal of Geophysical Research*, *101*(B12), 28291–28314.

Wijns, C., Weinberg, R., Gessner, K., & Moresi, L. (2005). Mode of crustal extension determined by rheological layering. *Earth and Planetary Science Letters*, *236*(1), 120–134.

Wilks, K. R., & Carter, N. L. (1990). Rheology of some continental lower crustal rocks. *Tectonophysics*, *182*(1–2), 57–77.

Zalán, P. V., Severino, M. D. C. G., Rigoti, C. A., Magnavita, L. P., Oliveira, J. A. B., & Vianna, A. R. (2011). An entirely new 3D-view of the crustal and mantle structure of a South Atlantic passive margin–Santos, Campos and Espírito Santo Basins, Brazil. In *AAPG annual conference and Exhibition* (pp. 10–13). Tulsa, OK: American association of Petroleum Geologists.